CHEMICAL REVIEWS

Review

Cite This: *Chem. Rev.* XXXX, XXX, XXX–XXX

pubs.acs.org/CR

Nonclassical Applications of *closo*-Carborane Anions: From Main Group Chemistry and Catalysis to Energy Storage

S. P. Fisher,[†] A. W. Tomich,[†] S. O. Lovera,[†] J. F. Kleinsasser,[†] J. Guo,[‡] M. J. Asay,*[,§] H. M. Nelson,*[,§] and V. Lavallo*[,†]

[†]Department of Chemistry, University of California, Riverside, 501 Big Springs Road, Riverside, California 92521, United States

[‡]Department of Chemical and Environmental Engineering, University of California, Riverside, Riverside, California 92521, United States

[§]Department of Chemistry and Biochemistry, University of California, Los Angeles, California 90095, United States

ABSTRACT: Classically *closo*-carborane anions, particularly $[HCB_{11}H_{11}]^-$ and $[HCB_9H_9]^-$, and their derivatives have primarily been used as weakly coordinating anions to isolate reactive intermediates, platforms for stoichiometric and catalytic functionalization, counteranions for simple Lewis acid catalysis, and components of materials like liquid crystals. The aim of this article is to educate the reader on the contemporary nonclassical applications of these anions. Specifically, this review will cover new directions in main group catalysis utilized to achieve some of the most challenging catalytic reactions such as C−F, C−H, and C−C functionalizations that are difficult or impossible to realize with transition metals. In addition, the review will cover the utilization of the clusters as dianionic C σ-bound ligands for coordination chemistry, ligand substituents for coordination chemistry and advanced catalyst design, and covalently bound spectator substituents to stabilize radicals. Furthermore, their applications as solution-based and solid-state electrolytes for Li, Na, and Mg batteries will be discussed.

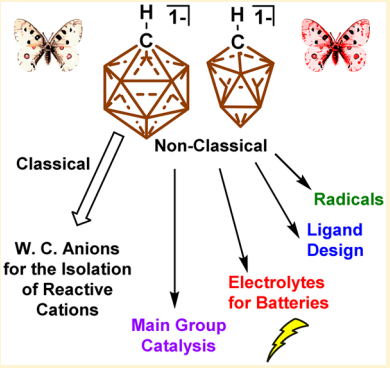

CONTENTS

1. INTRODUCTION

Since the pioneering work of Alfred Stock[1] and later Longuet-Higgins[2,3] and William Lipscomb,[4] borohydride clusters and their beautiful polyhedral shapes and unusual chemical bonding motifs have captivated the imagination of scientists. While some of these molecules are extremely pyrophoric, such as the notorious "green dragon" pentaborane B_5H_9,[5] others such as dianionic compounds $[B_{12}H_{12}]^{2-}$ (**1**) and $[B_{10}H_{10}]^{2-}$ (**2**) (Figure 1), first reported by Hawthorne,[6,7] are very thermally, chemically, and electrochemically stable species.[8−10] A vast

Special Issue: Frontiers in Main Group Chemistry

Received: September 4, 2018

DOI: 10.1021/acs.chemrev.8b00551
Chem. Rev. XXXX, XXX, XXX−XXX

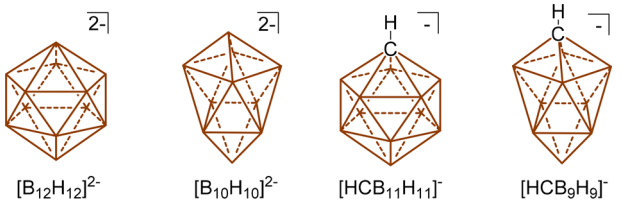

Figure 1. Most thermodynamically stable *closo*-dianionic borohydride and monoanionic carborane clusters **1**−**4** (unlabeled vertices = B−H).

subset of these species are carboranes,[11−20] where one or more of the vertices of the boron cluster have been replaced by carbon. Replacing a boron atom by carbon reduces the overall charge of the cluster by +1, as carbon has four valence electrons and boron has three. For example, the icosahedral **1** and square bicapped anti prism **2** have isoelectronic monoanionic carboranes $[HCB_{11}H_{11}]^-$ **3** and $[HCB_9H_9]^-$ **4**, respectively (Figure 1).[21] The official IUPAC names of **3** and **4** are 1-carba-*closo*-dodecaborate and 1-carba-*closo*-decaborate, respectively.[22] The aforementioned compounds **1**−**4** are termed *closo*-clusters as they have closed shell electronic structures and complete polyhedral shapes.[13] While often termed σ-aromatic, the molecular orbitals of these clusters are composed of both strongly bonding purely σ- and π-type overlaps, resulting in enormous HOMO/LUMO gaps. Similar to **1** and **2**, although more pronounced because of their monoanionic charges, the carborane anions **3** and **4** are inherently weakly coordinating as the charge of the cluster is delocalized throughout the three-dimensionally aromatic core.[15,20] Functionalization of these clusters surfaces with halogens or alkyl groups, through electrophilic aromatic substitution "like" reactions, renders these species even more weakly coordinating. The field of borohydride and carborane cluster chemistry is so vast that one review cannot contain a comprehensive assessment of the area. Indeed, many reviews[11,12,14−20,23] exist for subsets of these compounds and comprehensive books[24−26] have been published. While there are *closo*-carborane anions other than **3** and **4**, as outlined in detail in Grimes's comprehensive book *Carboranes*,[13] these species are not readily accessible and/or too reactive for robust applications. This review is designed to focus on contemporary nonclassical applications of *closo*-carborane anions **3** and **4**. The basic structure and bonding, synthesis, and library of known derivatives containing **3** have been reviewed elsewhere.[15] We define nonclassical applications as uses beyond coordination chemistry of the ionic bonding and σ-type complexation of the anions themselves,[27−33] weakly coordinating anions to isolate reactive intermediates,[20] weakly coordinating anions for Lewis acid catalysis,[34−42] anions for Li^+-initiated olefin polymerization,[43] liquid crystals,[17] and the catalytic functionalization of the cage vertices.[11] Specifically, this review will cover new directions in main group catalysis utilized to achieve some of the most challenging catalytic reactions such as C−F, C−H, and C−C functionalizations that are difficult or impossible to realize with transition metals. In addition, the review will cover the utilization of the clusters as dianionic C σ-bound ligands for coordination chemistry, ligand substituents for coordination chemistry and advanced catalyst design, covalently bound spectator substituents to stabilize radicals, and components for energy storage applications [electrolytes for rechargeable batteries (secondary batteries)].

2. CARBORANE ANIONS IN MAIN GROUP CATALYSIS

2.1. Silylium Carboranes

The silylium cation $[SiR_3]^+$ was a popular, if elusive, target for main group chemists from the 1990s into the 2000s and one that was no stranger to controversy. The first reports of a free silylium ion led to extensive discussions on the nature of secondary interactions and what could actually be classified as "free".[44−47] While a complete treatment of the history of silylium species is worth a perusal, it lies outside the scope of the current discussion and has been reviewed elsewhere.[48,49] What is relevant is that to even approach true silylium status, extremely noncoordinating counterions are required. Carborane anions, particularly the halogenated carboranes $[HCB_{11}X_{11}]^-$ $\mathbf{3X_{11}}$ and $[HCB_{11}H_5X_6]^-$ $\mathbf{3X_6}$ (X = Cl, Br, or I) have proven to be particularly useful in this regard (Figure 2).[26,50,51] Fluorinated derivatives of **3** are known

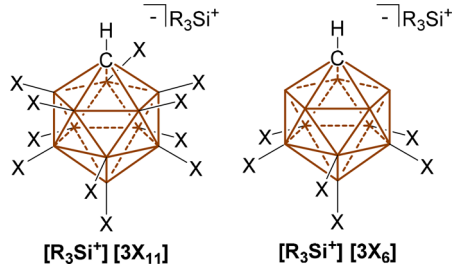

Figure 2. Silylium carboranes $[\mathbf{R_3Si^+}][\mathbf{3X_{11}}]$ and $[\mathbf{R_3Si^+}][\mathbf{3X_6}]$ used as catalysts (X = Cl, Br, or I; unlabeled vertices = B−H).

but require the use of HF/F_2 mixtures for their synthesis; thus, they have not found widespread utility. In addition to trivalent silicon cations, divalent aluminum species, alumenium cations, have also been generated and isolated as carborane salts, and although there has been less controversy surrounding these species, they are interesting molecules.[52,53] These main group cations remain fundamentally interesting, but much of the current interest in these species is focused on how their high reactivity can be harnessed for synthetic methods. To date, the applications of these cations have focused on their ability to activate inert bonds, specifically C−F and C−H bonds.[37,41,54−56] This section will detail these reactions.

The advantage of using carborane anions is twofold. First, the anionic charge is effectively dispersed throughout the cluster structure, which limits the interaction of the anion with highly charged cationic species, thus allowing them to maintain maximum reactivity. Second, the robust cluster bonding of the carborane cage renders them inert not only to the silylium itself but also to any high-energy, reactive intermediates generated in the course of the reaction. Where possible, the advantages of carborane anions over other weakly coordinating anions will be highlighted.

2.2. Catalytic Hydrodefluorination

Hydrodefluorination (HDF) chemistry, in the simplest terms, is the replacement of a fluorine with a hydrogen just as the name implies. Until relatively recently, this reaction received little interest probably because of the perceived synthetic difficulty of such a transformation as it involves the breaking of the strongest single bond to carbon, the C−F bond. Recently, fluorinated and partially fluorinated compounds have become increasingly relevant. Fluorinated hydrocarbons and related species, especially gaseous examples often used as refrigerants, have become a bane to the atmosphere and environment, which has

DOI: 10.1021/acs.chemrev.8b00551
Chem. Rev. XXXX, XXX, XXX−XXX

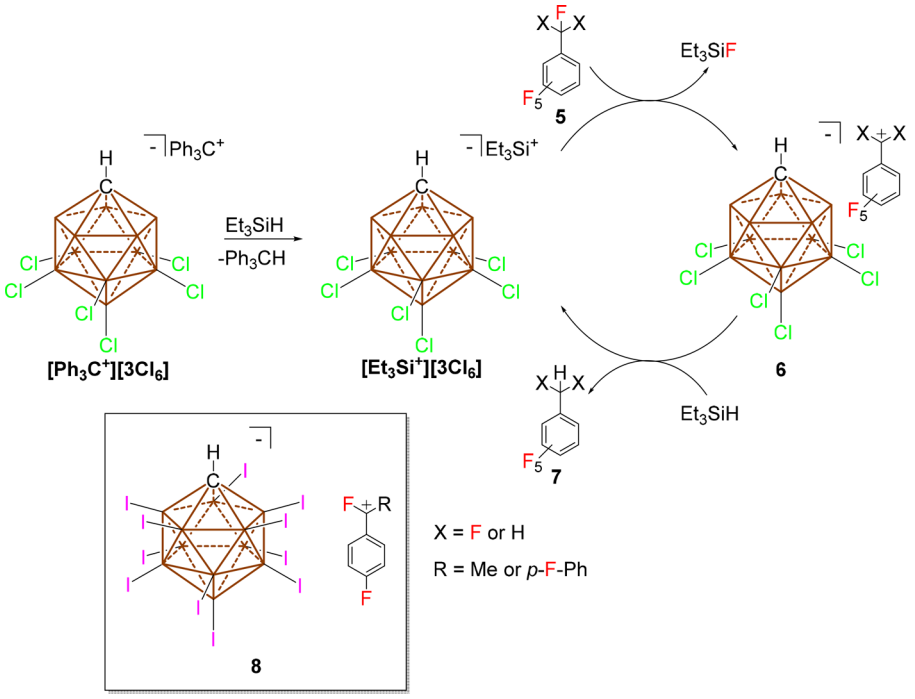

Figure 3. HDF catalytic cycle showing a single defluorination step, which is repeated iteratively until product **7** (X = H) is formed. The isolable fluorinated benzyl cation **8** is also shown.

led to increased interest in HDF protocols as a potential method for remediation.[57−60] Additionally, partially fluorinated compounds have garnered interest as active pharmaceutical ingredients.[61] One potential synthetic route to such fluorine-containing compounds is selective HDF of polyfluorinated precursors.

There has been some work on catalytic HDF involving the use of transition metal catalysts, importantly starting with the work of Milstein and co-workers with rhodium catalysts,[62,63] and this work has been summarized elsewhere.[64−70] Much of the metal-catalyzed chemistry still requires the use of a stoichiometric quantity of a main group compound that usually selectively reacts with aryl (sp^2) fluoride bonds.

The advent of isolable yet highly electrophilic/fluorophilic R_3Si^+ reagents highlighted the potential of such species in the activation of C−F bonds and the subsequent development of catalytic metal-free HDF reactions. In the simplest terms, one might suspect such a reaction is, at the very least, thermodynamically feasible by crudely comparing the bond energies of the broken and formed bonds [+565 kJ/mol (Si−F)/−485 kJ/mol (C−F); +411 kJ/mol (C−H)/−318 kJ/mol (Si−H) = 173 kJ/mol].[71−74] In this case, the naïve approach actually gives the correct result; however, much more detailed calculations have been done concerning the hydride and fluoride affinities of the relevant species. These calculations show that the hydride transfer is thermodynamically strongly favored while the fluoride transfer is at or around an energetically neutral process.

In 2005, Ozerov and co-workers reported the first silylium-mediated HDF reactions in which a catalytic amount of $[Ph_3C]^+[B(C_6F_5)_4]^-$ was used to generate the silylium $[Et_3Si]^+[B(C_6F_5)_4]^-$ in situ by addition of excess Et_3SiH (this is done largely for practical reasons, as the silylium cannot be stored for extended periods).[75,76] Trifluorotoluene derivatives were reliably hydrodefluorinated at room temperature with a tolerance for halide substituents on the arene. A single example of a primary alkyl fluoride was also converted with some difficultly; however, perfluorinated alkanes could not be converted, and polyfluoro alkanes were not reported. What is most germane to the current discussion is that the catalyst decomposes rapidly, which is responsible for the somewhat low turnover numbers (the best value reported being 126 when the reaction is run in pure trifluorotoluene). Indeed, $[B(C_6F_5)_4]^-$ can undergo aryl abstraction via reaction with highly reactive carbocations generated in situ, as evidenced by the formation of the borane $B(C_6F_5)_3$. The authors even note that "... activation of C−F bonds in perfluoroalkanes by this method remains elusive, it may yet be achieved via utilization of more robust counterions, such as halogenated carboranes ...",[75] which is exactly what they did.

Three years after the initial report, a similar protocol was implemented using $\mathbf{3X}_n$ carborane trityl salt precatalysts, such as $[\mathbf{Ph_3C^+}][\mathbf{3Cl_6}]$ (Figure 3).[77] They propose that the silylium cation $[\mathbf{Et_3Si^+}][\mathbf{3Cl_6}]$ abstracts a fluoride from the fluorinated substrate **5** to generate a benzyl carbocation **6**, which, in turn, abstracts a hydride from the triethylsilane, thus regenerating the silylium and converting one C−F bond to a C−H bond in product **7** (Figure 3). The potential advantage of using carborane counterions in this chemistry was clearly demonstrated by the report that reaction of $[\mathbf{Et_3Si^+}][\mathbf{3I_{11}}]$ with benzyl fluorides led to fluoride abstraction and generation of stable benzyl cations **8** (Figure 3, bottom left).[78] The isolation of the proposed benzyl cation intermediate as a stable species clearly shows that the carborane anion is not apt to decompose and should be stable under the reaction conditions.

The importance of a truly inert counterion for the efficacy of the silylium-catalyzed reactions was then investigated using three carborane anions, $\mathbf{3Br_6}$, $\mathbf{3Cl_6}$, and $\mathbf{3Cl_{11}}$, and the originally reported $[B(C_6F_5)_4]^-$ anion. Specifically, all of the carborane initiators exhibited faster reactivity [turnover numbers (TONs) of 140−180] at 1 h (0.4 mol % catalyst loading), while the $[B(C_6F_5)_4]^-$ salt achieved only four turnovers (Table 1, entries 1−4). Importantly, after 24 h, the same carborane reactions

DOI: 10.1021/acs.chemrev.8b00551
Chem. Rev. XXXX, XXX, XXX−XXX

Table 1. HDF Results for Catalyst Selection and Substrate Scope[c]

Entry	$[Ph_3C]^+$ Initiator	Substrate	Mol%	Time (h)	TON
1	$[B(C_6F_5)_4]^-$	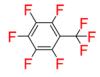	0.4	1	4
2	**3Cl$_{11}$** $[HCB_{11}Cl_{11}]^-$		0.4	1	180
3	**3Br$_6$** $[HCB_{11}H_5Br_6]^-$		0.4	1	140
4	**3Cl$_6$** $[HCB_{11}H_5Cl_6]^-$		0.4	1	180
5	**3Cl$_6$** $[HCB_{11}H_5Cl_6]^-$		0.1	1	875
6	**3Cl$_{11}$** $[HCB_{11}Cl_{11}]^-$		0.1	1	370
7	**3Br$_6$** $[HCB_{11}H_5Br_6]^-$		0.1	1	215
8	**3Cl$_6$** $[HCB_{11}H_5Cl_6]^-$		0.036	72	2700
9	**3Cl$_6$** $[HCB_{11}H_5Cl_6]^-$	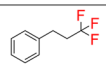	0.13	48	780[a]
10	**3Cl$_6$** $[HCB_{11}H_5Cl_6]^-$	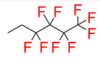	0.5	120	200[b]

[a]Performed neat or in benzene. [b]Performed neat at 50 °C using Hex_3SiH. [c]Reactions were performed at 25 °C in *o*-dichlorobenzene with Et_3SiH (1.1 equiv per C−F bond) unless otherwise stated. TON based on the number of consumed C−F bonds.

achieved >97% conversion while the $[B(C_6F_5)_4]^-$ system gave an only 6% yield. This study also highlighted an important feature of this reaction: The activity of the catalyst does not correlate to the basicity of the carborane ion. They found the activity increased from **3Br$_6$** to **3Cl$_{11}$**, with **3Cl$_6$** being the most active (Table 1, entries 5−7), while the basicity decreases from **3Br$_6$** to **3Cl$_6$**, with **3Cl$_{11}$** being the least basic.[51] The difference between the two more active carborane salts is significant, with **3Cl$_6$** achieving more than twice the number of turnovers in a single hour. Therefore, there may be important weak interactions between key intermediates and the carborane anion that lead to better and/or more stable catalysis, or more simply, the differences in activity may be related to different solubilities of the intermediate silylium/carbocations.

After finding that **3Cl$_6$** provided the most active catalytic system, they were able to achieve 2700 turnovers of this reaction at room temperature with a catalyst loading of only 0.036 mol % (Table 1, entry 8). Additionally, while the $[B(C_6F_5)_4]^-$ catalyst was reported to operate on only benzylic fluorides, the carborane salts successfully hydrodefluorinated the alkyl groups of both $PhCH_2CH_2CF_3$ and nonafluorohexane (Table 1, entries 9 and 10, respectively). To further emphasize the relative stability of the carborane catalysts, the latter case required moderate heating (50 °C) and still reached >97% conversion of the C−F bonds. They also changed from Et_3SiH to Hex_3SiH to increase the solubility of the silylium salt in the nonpolar reaction medium (the reaction was performed in neat nonafluorohexane), thus demonstrating the potential variability of the catalytic system.

These HDF results were promising, but as always, there are several caveats. The high reactivity of the carbocation intermediates means that the selectivity of the products formed depends on the starting material and solvent used in the reaction. For example, Friedel−Crafts-type products were obtained in the reaction of both $C_6F_5CF_3$ and $PhCH_2CH_2CF_3$, while four products were identified in the HDF of nonafluorohexane (Scheme 1). One of the better solvents for the HDF reaction was proven to be *o*-dichlorobenzene because of its unreactive bonds and reasonable polarity. However, in the case of the HDF of $C_6F_5CF_3$, only 53% of the strictly HDF product $C_6F_5CH_3$ **9** was found with 32% being the two isomers of $C_6H_3Cl_2-CH_2C_6F_5$ (**10** and **11**), formed by attack of the solvent on the carbocation intermediate followed by H_2 elimination. Importantly, ^1H nuclear magnetic resonance (NMR) of reaction mixtures had observable quantities of H_2, which gives credence to the proposed Friedel−Crafts reactivity. When the reaction was performed under neat conditions, Friedel−Crafts products were avoided and the $C_6F_5CH_3$ product was the only major product and isolated in 86% yield. The opposite was true for $PhCH_2CH_2CF_3$, which gave only 5% indane **12** (the intramolecular Friedel−Crafts product) as an isolable product when the reaction was performed under neat conditions. By using benzene as the solvent, the intermolecular reaction was favored and 1,3-diphenyl propane **13** was isolated as the major product (76%). Finally, the nonafluorohexane suffers from a different problem of selectivity. The expected *n*-hexane **14** was the major product formed in the reaction (28%) along with dimethylbutane **15** (most likely the result of intramolecular rearrangements of the alkyl cation intermediates), methyl cyclopentane **16**, and cyclohexane **17**. It is

Scheme 1. HDF Products of the Studied Substrates

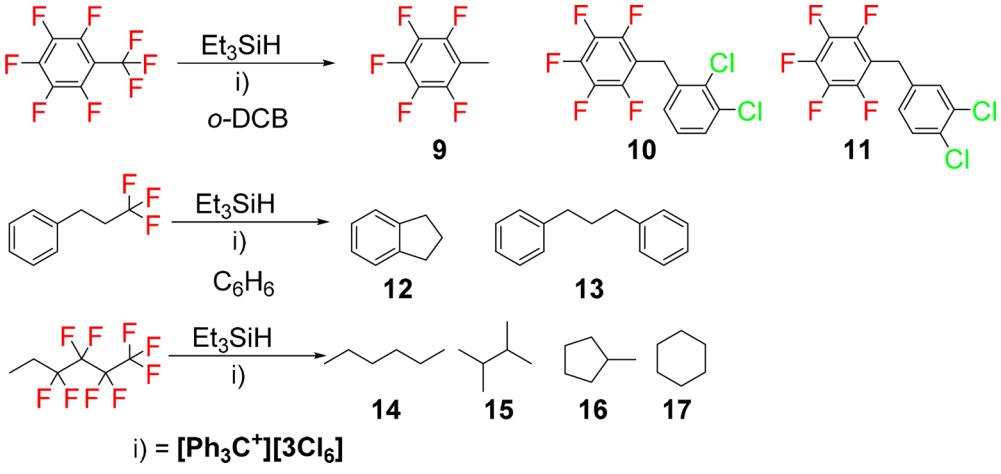

DOI: 10.1021/acs.chemrev.8b00551
Chem. Rev. XXXX, XXX, XXX−XXX

Scheme 2. Arene Fluoride Abstraction

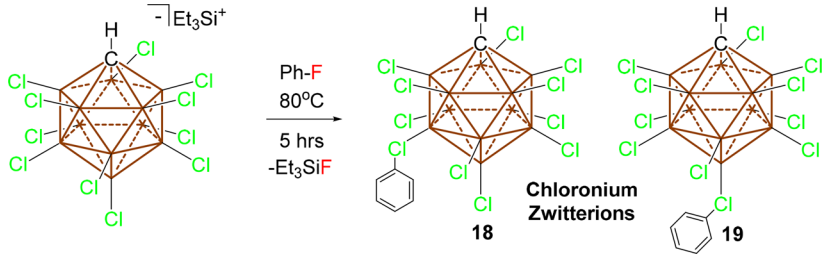

important to note that despite the formation of several products, all of the products have been completely defluorinated.

Subsequently, further investigation was done into the scope of the reaction, including more examples of alkyl monofluorides, which proved to be successful but difficult.[79] Attempts to hydrodefluorinate CF_4 were unsuccessful, even with high catalyst loadings. The $\mathbf{3I_6}$ anion was also investigated and proved to be less active than all of the other carboranes. Finally, the scope was expanded into hydrodechlorination, debromination, and deiodination of benzyl and alkyl halides. In the former case, hydrodechlorination occurs more readily than HDF; in the latter case, HDF is significantly faster and both processes are faster than hydrodebromination. The hydrodeiodation reaction was less studied, and while it appears to work, the inutility of such a reaction means the details were limited.

Some further modifications to the counterion have been made in an effort to improve the effectiveness of the silylium carborane catalyst. The carborane has been modified with a 12-triflate group $\mathbf{3Cl_{10}OTf}$, which was then used in HDF chemistry, and the activity was compared to that of $\mathbf{3Cl_{11}}$, with unfortunately unfavorable results.[80] The new catalyst had a TON of only 40 with a catalyst loading of 0.5 mol % on $C_6F_5CF_3$, a substrate that $\mathbf{3Cl_{11}}$ catalyzes with great efficiency (TON of 2000, 0.05 mol %, and >97% C−F conversion). Even with a more active substrate (*p*-fluoro-trifluoromethylbenzene), the triflate-substituted carborane underperformed (TON of 1700) versus the perchlorinated carborane (TON of 2000 at 0.05 mol %). Studies of the silylium carborane catalyst found that the triflate acted as a Lewis base to stabilize the cationic silicon center, and the leap to attributing this interaction to the loss of activity is quite small. The carborane cluster has also been exchanged for the parent dianionic *closo*-borane cluster **1**, and $[\mathbf{Ph_3C^{2+}}]_2[\mathbf{1Cl_{12}}]$ was used as the precatalyst.[81] The results were similar to some of the carborane results with turnover numbers of ≤2040 (based on the mole percent of the precatalyst and not the mole percent of silylium) for the *p*-F-C_6H_4-CF_3 substrate. A high TON (1920) was also possible for the more difficult perfluoro toluene substrate with an increase in the temperature of the reaction to 80 °C. The hexachloro catalyst remains the state of the art, but these results demonstrate that any sufficiently inert counterion may have application.

There have been some efforts to manipulate the cationic portion of the catalytically active ion pair. In the case of the carboranes, this has been limited to the use of different trialkyl silanes (Et_3SiH, Hex_3SiH, and iPr_3SiH). Disilyl cations have been used with the $[B(C_6F_5)_4]^-$ anion, which, as noted above, is not stable under the reaction conditions and therefore results in a low TON (45 for the HDF of fluorodecane).[82] Similarly, a dialkyl alumene cation $[^iBu_2Al]^+[B(C_6F_5)_4]^-$ gave a maximum TON of 60 for the HDF of trifluorotoluene.[83] Finally, dicationic phosphines have been used in HDF chemistry again using the $[B(C_6F_5)_4]^-$ anion.[84,85] High yields were obtained with a variety of substrates, but high catalyst loadings (5−10 mol %) again mean that these species are much less active than the carborane silylium species discussed above. However, all of these examples represent an important move toward main group element catalysis.

This section has highlighted the recent work in hydrodefluorination chemistry using silylium cations with unreactive carborane counterions. The robust cluster bonding of the halogenated carborane cages is resistant to decomposition and makes high-turnover catalysts possible. Implementation of these counterions with other systems may lead to further advancements in this area as more broadly applicable catalysts are sought with every increase in reactivity and/or selectivity. It is also important to note that this main group-catalyzed chemistry is complementary to the HDF done with transition metals as the former targets sp^3 carbons and the latter almost exclusively activates sp^2 carbons. The development of both domains will lead to valuable synthetic tools for the remediation of environmentally damaging fluorocarbons and the selective HDF of other targets.

2.3. Carbon−Carbon Bond-Forming Reactions

The HDF chemistry discussed above is extremely relevant, and new applications will surely be developed in the coming years; however, the replacement of a hydrogen with a fluorine remains a niche application in the larger domain of chemical synthesis and primarily serves as an end step process that does not add complexity. The formation of carbon−carbon bonds, on the other hand, is a ubiquitous process that serves to increase complexity and is applied at every level of synthesis. One of the targets of inorganic chemists has been molecular main group species that can serve as catalysts for such transformations. The primary advantages are the general abundance of main group elements and the environmentally and biologically benign nature of elements such as silicon and boron. Main group species have proven to be valuable catalysts for activating bonds via Lewis acid/base interactions, but their use as reactive centers for bond-breaking and/or -forming processes is much more rare.[86−88] This section will focus on the reported examples of the silylium carborane as a catalyst for carbon−carbon bond formation.

The potential of silylium carboranes to form new carbon−carbon bonds was demonstrated in the HDF chemistry in which Friedel−Crafts products were obtained by the reaction of the intermediate alkyl cations on aromatic solvent molecules. The only disadvantage of this protocol is the use of the complicated and air/moisture sensitive carborane silylium species for a job that $AlCl_3$ does with striking simplicity and efficiency (although not catalytically).[89,90] However, this would change with Reed and Siegals's report of aryl C−F activation by a silylium carborane.[91] Heating a fluorobenzene solution of $[\mathbf{Et_3Si^+}]$-

DOI: 10.1021/acs.chemrev.8b00551
Chem. Rev. XXXX, XXX, XXX−XXX

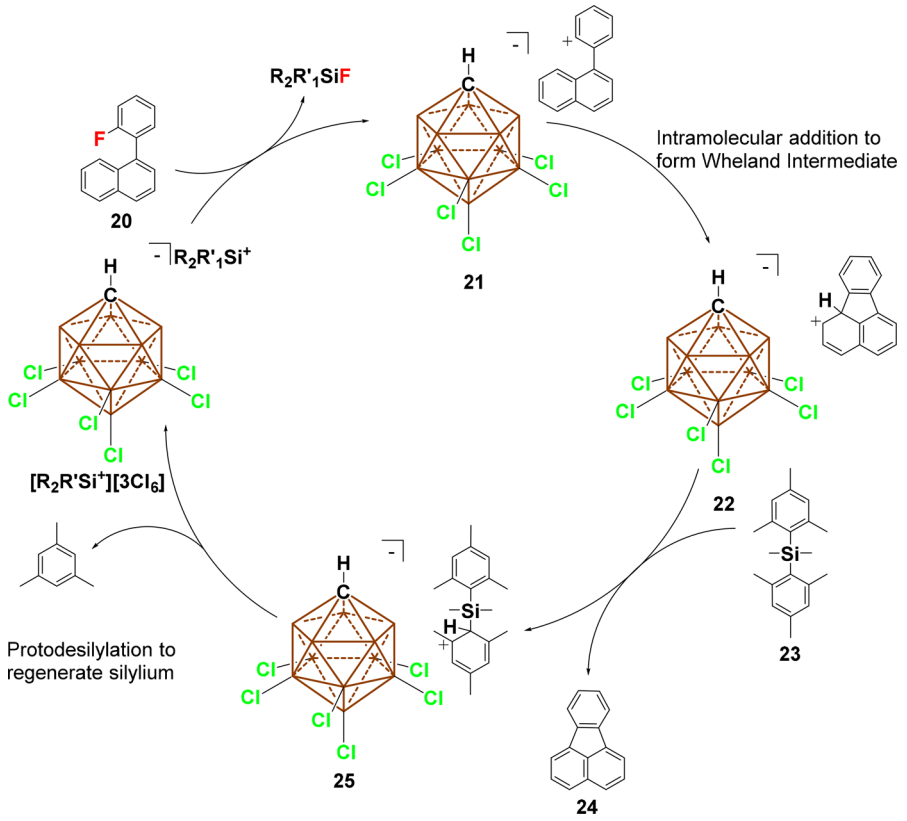

Figure 4. Catalytic cycle for the intramolecular Friedel−Crafts arylation reaction catalyzed by silylium carboranes.

$[\mathbf{3Cl_{11}}]$ to 80 °C led to the isolation of the 7- and 12-chloronium zwitterions **18** and **19**, respectively (Scheme 2).

The abstraction of fluoride from an aryl group was an important observation. Furthermore, the authors observed fluorobiphenyl products, albeit in small quantities, were generated in the reaction. These products could be the result of Friedel−Crafts-type reactivity of two aryl groups, which is impossible with $AlCl_3$. This observation led to the subsequent report of the intramolecular coupling of aryl fluorides with a silylium carborane catalyst.[92] One equivalent of HF is generated in the reaction, and therefore, a base can be used as a proton sponge with the fluoride being accepted by the silylium. However, to get the reaction to turn over catalytically, an aryl silane (Me_2SiMes_2) is added, which acts as a proton acceptor and regenerates the silylium catalyst by protodesilylation. With these steps in mind, a catalytic cycle could be proposed (Figure 4). If $[\mathbf{R_2R'Si^+}][\mathbf{3Cl_{11}}]$ (R = Me; R′ = Me) is used as a catalyst, it first abstracts the fluoride from the substrate **20** to generate the phenyl cation carborane **21**. The phenyl cation is then attacked intramolecularly by the π-system of the adjacent naphthyl to form Wheland intermediate **22**, which is sufficiently acidic to protonate the Me_2SiMes_2 **23** and eliminate the product **24**. The protonated silane **25** undergoes protodesilylation to eliminate mesitylene and regenerate the silylium $[\mathbf{R_2R'Si^+}][\mathbf{3Cl_{11}}]$ (R = Me; R′ = Mes). As indicated by the chloronium chemistry (vide supra), this required an elevated temperature (110 °C) and the catalyst loading was significant (10 mol %) but yields of >90% were obtained. Interestingly, only the $\mathbf{3Cl_6}$ anion was reported, despite the fact that the silylium salt of $\mathbf{3Cl_{11}}$ activates the aryl C−F bond at 80 °C (silylium salts of $\mathbf{3Br_6}$ and $\mathbf{3Cl_6}$ were not reported to generate their halonium analogues in heated F−C_6H_5 solutions). The reasoning for the selection of carborane has not been reported. However, the borate $[B(C_6F_5)_4]^-$ was assayed and found to give no discernible yield of the desired product. This again demonstrates the utility of the extremely robust and inert carborane cluster as a weakly coordinating anion for transformations involving highly electrophilic intermediates.

The utility and novelty of this arene coupling Friedel−Crafts reaction are evident, but there are a variety of limitations. An intermolecular version of this reaction would be a very useful tool for synthetic chemists. The intramolecular reaction does have a limited scope as well inasmuch as alkyl substituents can cause side reactions via alkyl C−H insertion reactions.[93] However, as we will see, these problems can be overcome by the perspicacious choice of aryl cation source.

The extreme reactivity of the aryl cation is at the heart of the lack of selectivity of the aforementioned reactions. One excellent method for stabilizing cations is the β-silyl effect, and therefore, Nelson and co-workers targeted *o*-silyl fluorobenzenes as precursors to β-silyl phenyl cations. Additionally, the silyl substituent should enhance the nucleophilicity of the π-system, which, in turn, would enhance the insertion reactivity of the aryl cation. Finally, the silyl group can serve as the mechanism for turnover of the reaction and generation of a catalytic cycle. With these experimental design parameters in mind, TMS-substituted fluoroarenes were treated with silylium carboranes in the presence of a variety of alkanes and arenes. The desired arylated products were generated in yields of ≤99% with catalyst loadings of 2−5 mol %.[94] The most convenient methodology uses the trityl carborane as a precatalyst, which generates the silylium upon addition of an appropriate silane (Et_3SiH or iPr_3SiH). The silane is added in substoichiometric quantities (4−10 mol %) because the eliminated trimethylsilylium acts as a catalyst after

DOI: 10.1021/acs.chemrev.8b00551
Chem. Rev. XXXX, XXX, XXX−XXX

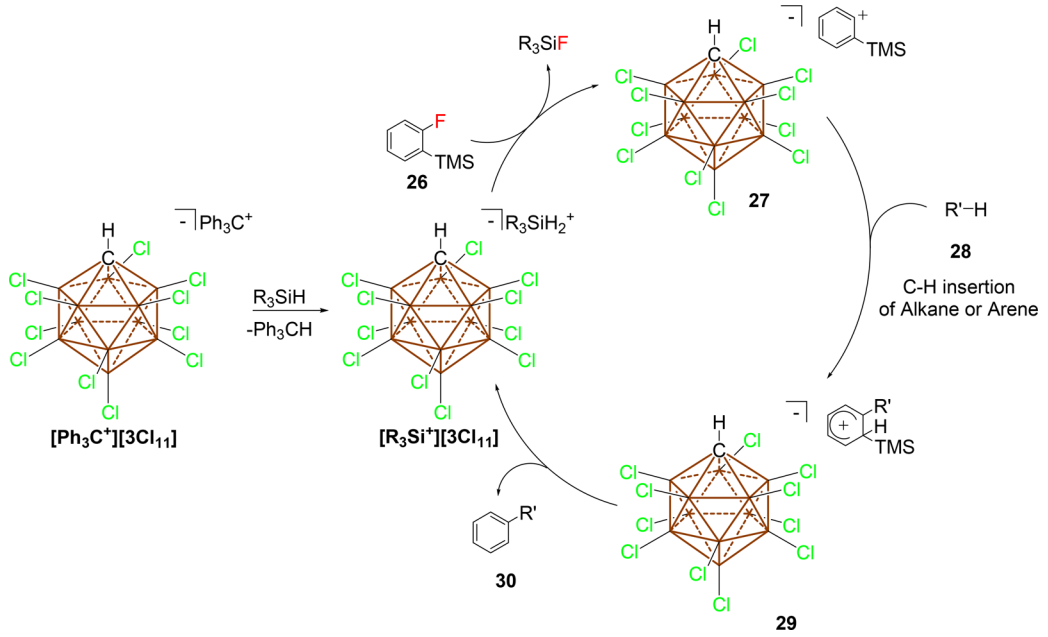

Figure 5. Catalytic cycle for the arylation of hydrocarbons using silylium carboranes.

the first catalytic cycle. This can be seen in the proposed catalytic cycle (Figure 5), wherein the initiation step involves the use of $[\mathbf{Ph_3C^+}][\mathbf{3Cl_{11}}]$ to generate silylium $[\mathbf{R_3Si^+}][\mathbf{3Cl_{11}}]$ by hydride abstraction. Subsequently, abstraction of fluoride from **26** forms the β-silyl-stabilized aryl cation **27**. This aryl cation is sufficiently stable and π-basic to undergo a 1,2-insertion reaction with the substrate **28** (R′ = alkyl or aryl) to form the arenium intermediate **29**, which eliminates the $[\mathbf{R_3Si^+}][\mathbf{3Cl_{11}}]$ (R = Me) catalyst and generates the target-functionalized product **30**.

The scope of the reaction spans simple alkanes (methane) to secondary cyclic alkanes and does prefer reaction at the primary position of straight chain alkanes. Only benzene has been reported as a coupling partner for the arene system, but a variety of substituents on the aryl fluoride have been probed, including other halogens, aryl groups, and alkyl chains (Table 2). Additionally, mechanistic studies were performed to demonstrate the likely formation of the aryl cation intermediate. Importantly, the carborane counterion is the choice of a weakly coordinating counterpart to the silylium. In this case, all reactions are performed with the $\mathbf{3Cl_{11}}$ counterion. Again, this carborane has proven to be one of the least basic counterions and one of the most inert; furthermore, it is the anion that was used to generate Reed and Siegels's chloronium zwitterions, which were generated via phenyl cation intermediates. Indeed, some reactions were functional at only 30 °C, which demonstrates the superior defluorination ability of $[\mathbf{R_3Si^+}][\mathbf{3Cl_{11}}]$ and the stabilizing effect of the β-silyl substituent.

The implementation of kinetically persistent phenyl cations in C−H bond activation processes using silylium carborane catalysts led to the investigation of other dicoordinate cations with similar chemistry. Vinyl cations make up a less examined class of reactive intermediates but, considering the reactivity described above, may have the ability to insert into C−H bonds. This, of course, requires the generation of the cationic species in a suitably mild manner, such that intermolecular reactions are possible and such that the counterion does not interfere with the high-energy intermediates. The solution to both of these problems is the use of a silylium carborane salt, specifically $[\mathbf{R_3Si^+}][\mathbf{3Cl_{11}}]$. The silylium cation was found to abstract triflate

Table 2. Arylation of Hydrocarbons Enabled by $[\mathbf{Ph_3C^+}][\mathbf{3Cl_{11}}]$ and $\mathbf{R_3SiH}$[b]

Ar-F	Substrate	Temp.(°C)	Time(h)	Product	Yield(%)
		70	1		54
	Pentane	60	8	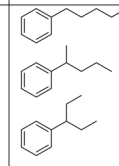	30 42 10 2
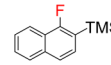	Methane	60	24		32[a]
		30	1		49
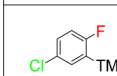		70	9	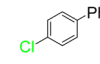	47
		30	0.2		99
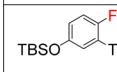		60	36	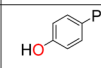	36

[a]Methane pressure of 35 bar using $[\mathbf{Et_3Si^+}][\mathbf{3Cl_{11}}]$ (3.6 mol %) as the catalyst. [b]Substrate and conditions for the arylation of hydrocarbons using the $[\mathbf{Ph_3C^+}][\mathbf{3Cl_{11}}]$ initiator (2 or 5 mol %) and R_3SiH (R = Et or iPr, 4 or 10 mol %) in *o*-DCB unless otherwise noted.

(trifluoromethanesulfonate, OTf) from vinyl triflate species, which if done in the appropriate aliphatic solvent would lead to the desired alkyl C−H insertion products. For example,[95] the $[\mathbf{Ph_3C^+}][\mathbf{3Cl_{11}}]$ salt could once again be used as a precatalyst (2 mol %), which in the presence of Et_3SiH generates the

DOI: 10.1021/acs.chemrev.8b00551
Chem. Rev. XXXX, XXX, XXX−XXX

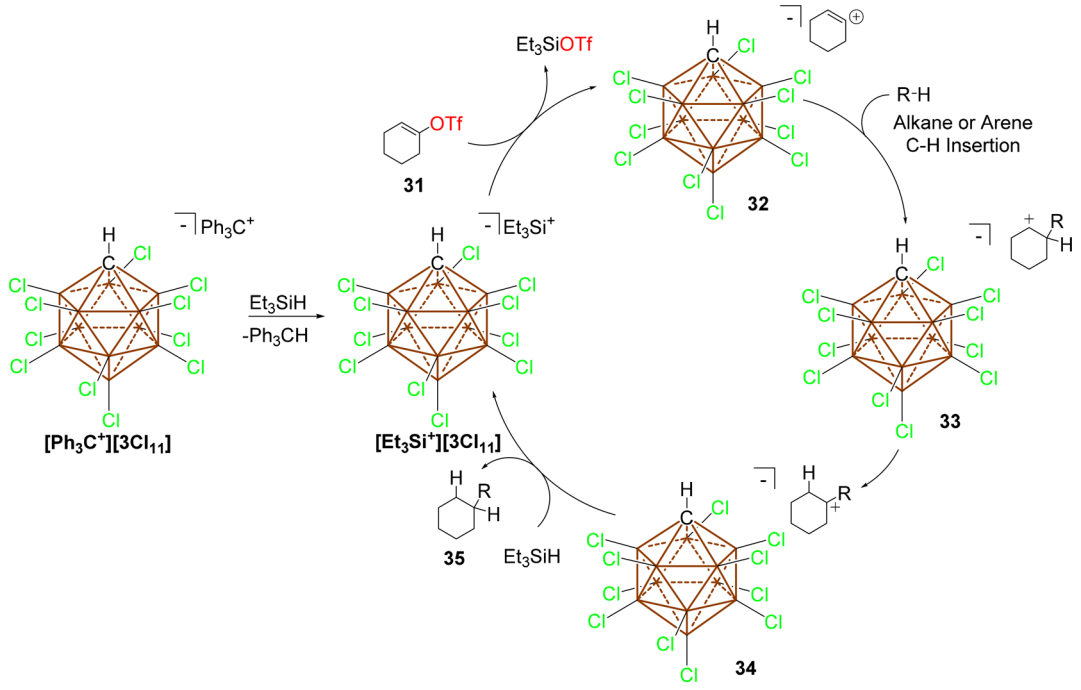

Figure 6. Catalytic cycle for the intermolecular C−H insertion reaction of vinyl cations catalyzed by $[\mathbf{Et_3Si^+}][\mathbf{3Cl_{11}}]$.

catalytically active $[\mathbf{Et_3Si^+}][\mathbf{3Cl_{11}}]$. The silylium abstracts the triflate from cyclohexenyl triflate **31** to generate the reactive vinyl cation carborane salt **32**. This cation then inserts into the C−H bond of the substrate generating the secondary carbocation **33**, which undergoes a 1,2-hydride shift to give the tertiary carbocation **34**. Similar to the trityl cation, **34** abstracts the hydride from Et_3SiH to regenerate the silylium carborane catalyst $[\mathbf{Et_3Si^+}][\mathbf{3Cl_{11}}]$ and the product **35** (Figure 6). The ease with which the silylium abstracts the triflate is evident by the low temperatures required for many of the reactions (−40 to 70 °C). The reaction is competent for a variety of cyclic and acyclic vinyl triflates and couples them with cyclic and straight chain alkanes as well as aryl groups (Table 3). There are several challenges that remain with this reactivity because of the highly reactive vinyl cation species. Noncyclic coupling partners can lead to mixtures of isomers, and currently, the substrate scope is limited to unsubstituted alkanes and halo-substituted aryls. The product mixtures led to significant investigation of the mechanism both theoretically and experimentally. The conclusion is that the reaction proceeds by a nonclassical cation intermediate, which is responsible for the mixtures of isomers on the vinyl triflate (i.e., addition at both carbons of the alkene). This reaction is once again feasible using only the appropriate carborane anion and was not reported to work with simpler more reactive weakly coordinating anions.

In this section, new carbon−carbon bond-forming reactions have been discussed, all of which feature silylium cations in essential activation steps that generate reactive cationic intermediates. These reactions are highly important because of the rarity of C−C bond-forming reactions available to synthetic chemists. Additionally, all of the reactions feature C−H functionalization chemistry, which remains rare in all domains of chemistry. All of this chemistry is made possible by the carborane cluster, which does not decompose under the reaction conditions. Even so, numerous challenges in the field remain, including functional group tolerance, complicated by the Lewis acidic silylium, which, for example, is quenched in the presence

Table 3. Examples of the Catalytic C−H Insertion Reaction of Vinyl Cations under Silylium Carborane Conditions[c]

Vinyl Triflate	Substrate	Time (h)	product	Yield (%)
		1.5		87
	Pentane	2	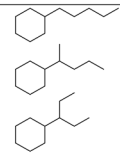	21 68 36 11
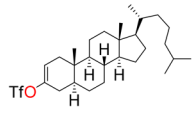		3	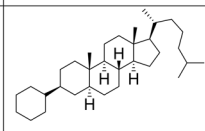	88[a]
		2	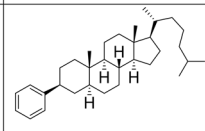	90[b]
		6		85
		1	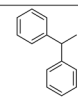	77

[a]The isolated dr is 15:1. [b]The isolated dr is 8:1. [c]The reactions were performed at 30 °C with $[\mathbf{Ph_3C^+}][\mathbf{3Cl_{11}}]$ as an initiator (2 mol %) and R_3SiH (R = Et or iPr, 1.5 equiv).

DOI: 10.1021/acs.chemrev.8b00551
Chem. Rev. XXXX, XXX, XXX−XXX

of basic functional groups. Additionally, such high-energy and reactive intermediates, such as phenyl and vinyl cations, lead to difficulties in obtaining highly selective fuctionalization products over a broad scope of substrates. However, the further elucidation of this type of chemistry has enormous potential to lead to new and valuable synthetic tools for the creation of complex molecules from relatively simple starting materials, by functionalization of some of the most basic bonds, C−H bonds.

2.4. Alumenium Carborane Catalysis

The halophilicity of aluminum species is well reported and responsible for the efficacy of Friedel−Crafts chemistry and the use of methylaluminoxane (MAO) as an initiator in polymer chemistry. Shortly after the report of the first silylium-catalyzed HDF reaction, an alumenium cation $[^{i}Bu_2Al]^+[B(C_6F_5)_4]^-$ was reported to be an operational catalyst in this transformation but with inferior activity compared to that of the best silylium carborane results (vide supra).[83] However, the ability of alumenium cations to abstract fluorides from alkanes indicates their potential as fluoride abstraction reagents.

The first application of an alumenium carborane cation appeared a number of years later and took advantage of the polar C−Al bond to generate new C−C bonds using trialkylalumanes. In this case, the R_3Al (R = Me, Et, or iBu) reagents were reacted with $[\mathbf{Ph_3C^+}][\mathbf{3Br_6}]$ to generate the desired $[\mathbf{R_2Al^+}][\mathbf{3Br_6}]$ catalyst (the catalysts could also be generated in situ).[96] The alumenium abstracts the fluoride from *p*-fluoro-trifluorotoluene **36** to give the corresponding benzylic cation, which accepts alkyl group transfer from the trialkylalumane to give the trialkyl products **37** (Figure 7). The alkyl group transfer also regenerates

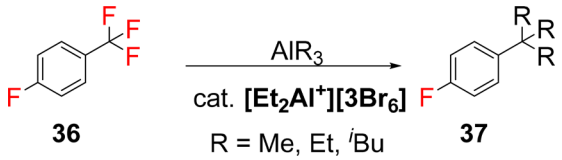

Figure 7. Alkyl defluorination reaction catalyzed by a cationic alumenium carborane salt.

the alumenium carborane catalyst $[\mathbf{R_2Al^+}][\mathbf{3Br_6}]$ and thus turns over the catalytic cycle, which is analogous to the silylium HDF cycle (see Figure 3). This system was also able to catalyze the HDF chemistry if iBu_2AlH was used in lieu of the trialkylalumane (although some alkylated product was observed in the reaction mixture). In every case, all of the fluorides are removed from the benzylic position, but with ethyl and butyl groups, mixtures of mono-, di-, and trialkylated products were observed with the remaining hydrides coming from the *β*-position of the alumane.

The reaction is tolerant to the presense of halide substituents on the aryl group as was observed for the HDF chemistry because the alumenium, like the silylium, does not readily dehalogenate the aryl group. However, the reaction does work with nonbenzylic alkyl fluorides. The functional group tolerance is limited once again by Friedel−Crafts chemistry; terminally fluorinated propylbenzene substrates first undergo intramolecular Friedel−Crafts chemistry to produce the difluorinated bicyclic system, which subsequently undergoes alkylation. Interestingly, this reaction operates with MAO as the aluminum alkyl source, which considering the availability of MAO, makes it quite convenient.

Alumenium carboranes[36,38,40] do appear to have interesting potential in catalytic reactions, and there have been some reports of their use in areas outside the scope of this review; however, as yet, their use has remained quite limited in HDF, alkyl defluorination, and other catalytic processes.

3. LIGANDS AND SYNTHESIS

Ligand design is an integral part of homogeneous catalysis and the architecture of tunable properties for many target materials. Classical ligand scaffolds are dominated by species that contain alkyl or aryl substituents. Soon after the discovery of the neutral icosahedral carboranes $H_2C_2B_{10}H_{10}$,[97−99] such clusters were heavily investigated as ligand substituents for phosphines as well as many other standard ligand classes.[14] To this day, however, there are no examples of catalysts supported by such ligands that surpass the activity and or selectivity of systems featuring classical hydrocarbon-appended ligands. This fact is perhaps due to the base sensitivity and ease of B−H cyclometalation of such $H_2C_2B_{10}H_{10}$ clusters, particularly the *ortho* isomer.[14] One notable exception for interesting reactivity, but not catalysis, is Bourissou's seminal report of a diphosphine featuring a $C_2B_{10}H_{10}$ backbone that facilitates the unusual oxidative addition to Au(I)[100] and allows for the isolation of elusive Au carbene complexes.[101] The unusual oxidative addition reactivity of this system was attributed to the constrained geometry of the ligand, which lowers the barrier for oxidative addition. There was also a report of a highly Z-selective olefin metathesis catalyst supported by a dithiolato *o*-carborane ligand, which was later retracted.[102]

Until recently, there have been few reports on the utilization of carborane anions **3** and **4** in ligand design, which is in stark contrast to the many publications about incorporation of $H_2C_2B_{10}H_{10}$ clusters. This is rather surprising given the superior chemical stability of **3** and **4**. The following sections will highlight the coordination chemistry of **3** and **4** as X_2-type ligands derived from the deprotonation of the C vertex of the clusters (X_2-type ligands = dianionic ligands with a negative charge at a cluster vertex and a second charge delocalized through the cage). In addition, we will highlight advances in ligand design, coordination chemistry, and catalysis where **3** and **4** are utilized as ligand substituents to form LX-type species (LX

Scheme 3. Isolable Dianionic Intermediates

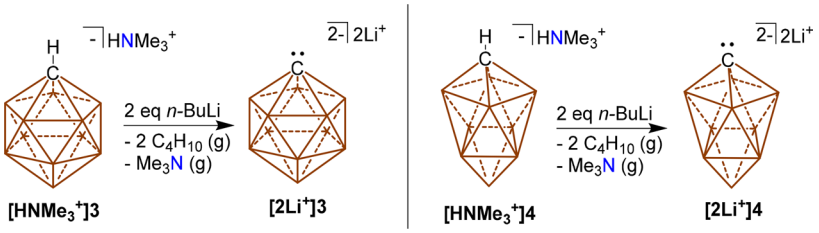

DOI: 10.1021/acs.chemrev.8b00551
Chem. Rev. XXXX, XXX, XXX−XXX

= a neutral ligand with a pendant charged carborane substituent that has the potential to be bidentate through secondary interactions with the cage surface groups). The coordination chemistries of **3** and **4** as weakly coordinating anions themselves are not included, and the reader is redirected elsewhere for studies of this topic.

3.1. X_2-Type Ligands

In the past 25 years, there have been only a handful of examples that utilize the *closo*-carborane monoanions as X_2-type ligands (X_2-type ligands = dianionic ligands with a negative charge at a cluster vertex and a second charge delocalized through the cage). These species are similar to phenyl anions but contain an extra charge because of the cluster core, which renders them dianionic. Synthesis of these complexes is often achieved by deprotonating the C−H vertex with a base generating the reactive but isolable dianionic *closo*-carboranes, [**2Li**$^+$]**3** and [**2Li**$^+$]**4** (Scheme 3). These carbanions can subsequently be transmetalated to transition metals or other electrophilic entities. Alternative strategies such as utilizing a transition metal with a built-in basic ligand to induce metalation are also possible, vide infra.

3.1.1. Group 11 Complexes. In 1998, Strauss and co-workers[103] reacted $[Cu(mesityl)]_n$ with $[(n\mathbf{Bu})_4\mathbf{N}^+][\mathbf{3F_{11}}]$ in methylene chloride resulting in no reaction. However, with the addition of $[N(n\text{-}Bu)_4]Cl$, as a source of Cl^-, the reaction produced **38** (Scheme 4). In the crystal structure, the Cl−Cu−

Scheme 4. Synthesis of Cu Complex 38

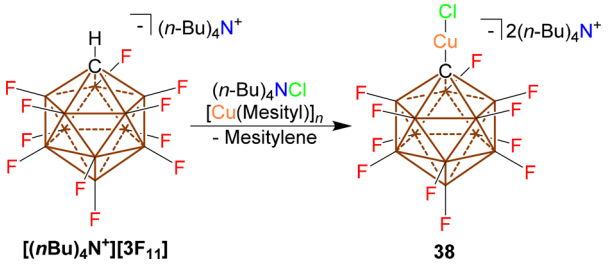

$C_{cluster}$ angle was nearly linear at 176.0°. Notably, there were no intra- or intermolecular contacts with the copper cation or the fluorine atoms of the carborane cluster.

Recently, Duttwyler and co-workers have reported the synthesis of a Cu complex in which the antipodal boron (B12) was appended with a cyano group.[104] Deprotonation of **39** with lithium tetramethylpiperidide (LiTMP) produced the dianion **40**. Compound **40** represents the first lithiated dianion studied by X-ray crystallography. This dianion was then reacted with CuI forming copper complex **41** (Scheme 5). Complex **41** was then used as a cuperate salt during the transmetalation of iodoarenes in palladium-catalyzed cross coupling.

The only report of a Ag complex with a σ-bound cluster via the C vertex was by Xie in 2003.[105] This was achieved by deprotonation of [**HNMe**$_3^+$][**3I**$_5$**Br**$_6$] with KOH in water followed by addition of $AgNO_3$ giving the trianionic metal complex **42** (Scheme 6). The crystal structure revealed three weakly coordinating Ag cations and one Ag cation C-bound to two **3I**$_5$**Br**$_6$ clusters. The complex was perfectly linear and contained a Ag−$C_{cluster}$ distance of 2.142(7) Å, which was slightly longer than the Ag−C distance of 2.097(9) Å for terphenyl $[Ag(C_6H_2\text{-}2,4,6\text{-}Ph_3)_2]^-[Li(THF)_4]^+$ or terphenyl $[Ag(C_6H_2\text{-}2,4,6\text{-}Ph_3)_2]^-[Li(THF)_4]^+$.[106]

Scheme 5. Synthesis of Cu Complex 41 and Isolated Li Salt 40

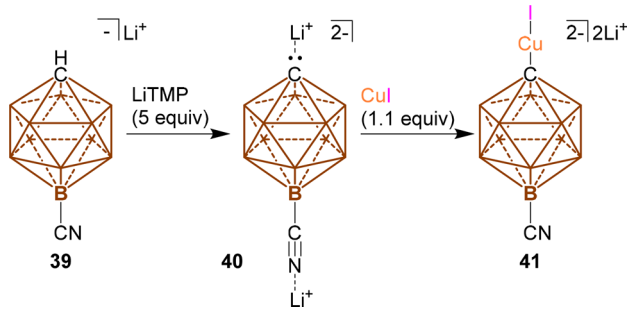

Scheme 6. Synthesis of Ag Complex 42

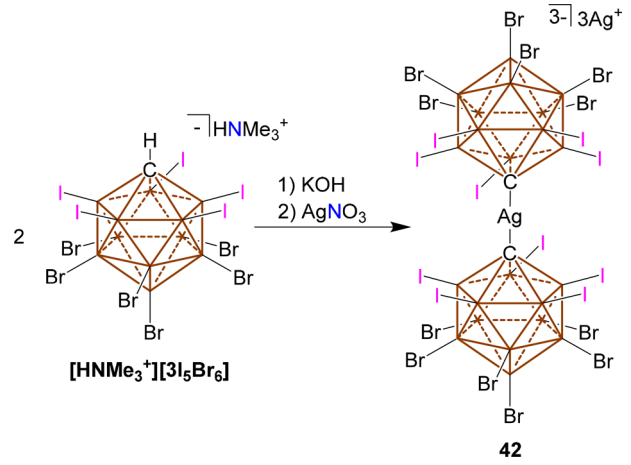

In 2009, Finze and co-workers released the first report detailing the metalation of the clusters **3** and **4** to Au (Scheme 7).[107] C-Lithiation of the cesium salts of **3** and **4** followed by treatment of the mixed Li^+/Cs^+ salts [**Li**$^+$**Cs**$^+$]**3** and [**Li**$^+$**Cs**$^+$]**4** with$ClAuPPh_3$ afforded the corresponding Au(I) anions **43** and **44**, respectively (Scheme 7, top). Unique to this paper is the parallel reactivity of the 2-isomer of **4**, compound **45** (Scheme 7, bottom). Paralleling the reactivity of **4**, **45** can also be deprotonated with *n*-BuLi yielding non-isolated dianionic intermediate **46**, which then undergoes metalation with Cl-Au-PPh_3 furnishing **47**. Thermal studies of **47** revealed that it isomerizes to the more stable **44** at 150 °C.

3.1.2. Group 12 Complexes. In 2011, Wehmschulte and Wojtas tested [**EtZn**(η^3-$\mathbf{C_6H_6}$)$^+$][**3Cl**$_{11}$] as an intramolecular hydroamination catalyst for the cyclization of $CH_2CHCH_2C(Ph_2)CH_2NHR$ (R = H or Ph).[108] The catalyst was competent for the cyclization of the secondary amine (R = Ph). However, the primary amine (R = H) showed no reactivity (Scheme 8). Incidentally, they observed catalyst decomposition to C−Zn metalated compound **48**. In the solid state, the Zn−$C_{cluster}$ distance was found to be 2.049(5) Å, which is only slightly longer than related cationic EtZn complexes.[109,110] This $C_{cluster}$−H deprotonation followed by metallization could be why compound **48** was catalytically inactive.

Finze and co-workers reported a systematic synthesis of $C_{cluster}$ mercurated derivatives of **3**. This was done by deprotonating an array of **3X**$_{11}$ (X = H, F, Cl, Br, or I) clusters with *n*BuLi, followed by addition of PhHgCl or $HgCl_2$ yielding a variety of **PhHg**[**3X**$_{11}$] and **Hg**[**3X**$_{11}$]$_2$ (X = H, F, Cl, Br, or I) complexes **49**−**53** and **54**−**58**, respectively (Scheme 9).[111,112] A majority of these compounds were characterized by multi-

DOI: 10.1021/acs.chemrev.8b00551
Chem. Rev. XXXX, XXX, XXX−XXX

Scheme 7. Synthesis of C−Au 10- and 12-Vertex Carborane Complexes

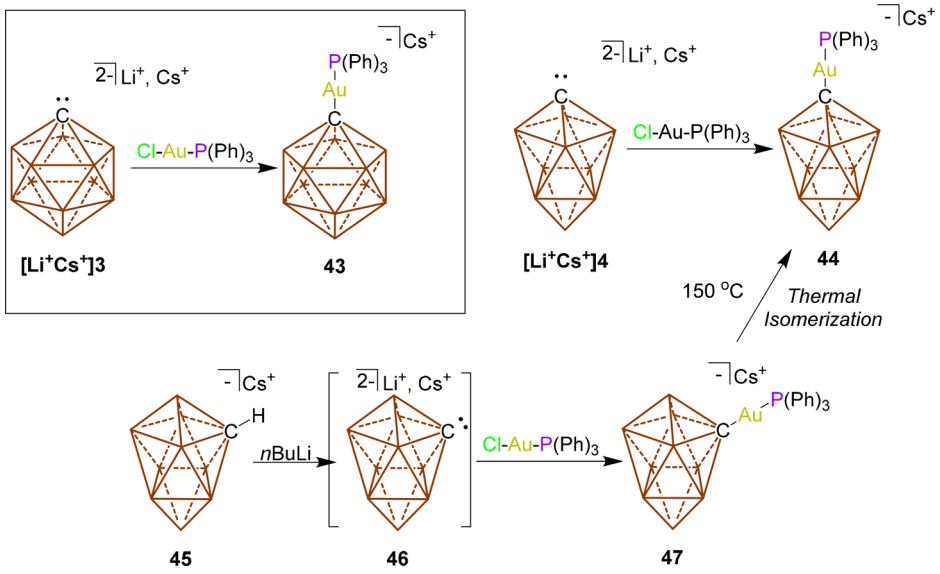

Scheme 8. Decomposition of Zn Catalyst to Complex 48

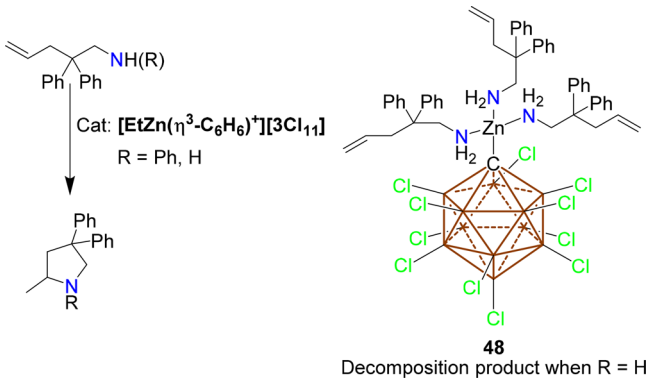

nuclear NMR, mass spectrometry, and elemental analysis, except for **53**, which was identified by only mass spectrometry. The $[Et_4N^+]$ salts of the fluorinated Hg(II) compounds (**51** and **55**) are air and water stable and have high thermal stability, not decomposing until 200 °C.

Cs^+ or Et_4N^+ salts of **49**, **50**, **52**, and **54**−**57** represent the first crystallographically characterized Hg-CB_{11} complexes. The $C_{cluster}$−Hg−C_{ipso} bond angles in **49**, **50**, **52**, **54**, **56**, and **57** are nearly all linear at >174°. However, this was not the case for **55**, which shows noticeable distortion from linearity due to a solvent molecule (H_2O or CH_3CN) coordinating to the electrophilic Hg(II) center inducing a pseudotrigonal planar geometry around Hg. This increased coordination was examined by density functional theory calculations, and it was determined that electronically, the halogenated species (**55**−**58**) should be able to form tricoordinated complexes. However, because of the increased steric demand of the halogens larger than fluorine, this coordination becomes unfavorable.

Continuing the study of bis(carboranyl)mercury(II) complexes, Finze and co-workers appended alkynyl fragments to the antipodal boron (B12) of the CB_{11} core, via a cross coupling methodology.[113] The Hg complexes were synthesized via two different synthetic strategies outlined in Scheme 10 generating **59**−**61**. Cyclic voltammetry and differential pulse voltammetry were performed on **59** to understand the compound's electrochemical properties. Cyclic voltammetry indicated one reversible oxidation at an $E_{1/2}(CH_3CN)$ of +0.04 V. The compound displays no electronic coupling between ferrocenyl fragments as indicated by a single redox event in CV and differential pulse voltammetry. The Hg(II) linkage at $C_{cluster}$

Scheme 9. Array of $C_{cluster}$ Mercuration Complexes

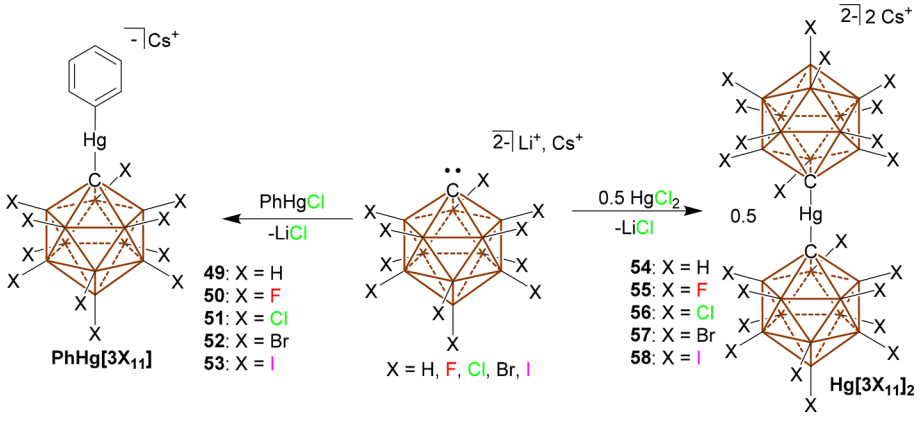

DOI: 10.1021/acs.chemrev.8b00551
Chem. Rev. XXXX, XXX, XXX−XXX

Scheme 10. Routes to $[Hg(12\text{-Alkynyl-1-}CB_{11}H_{10})_2]^{2-}$

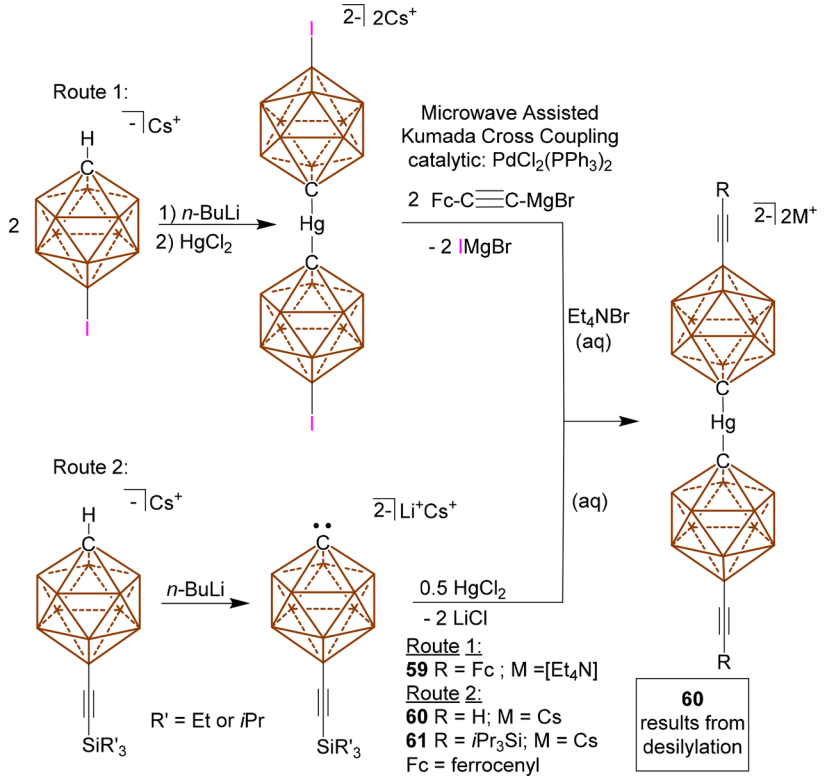

Scheme 11. Synthesis of Au Complexes 63−65

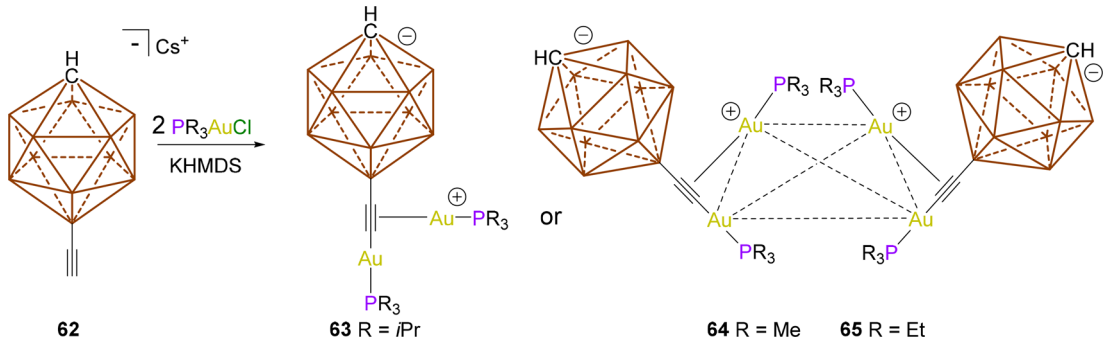

does not change the redox properties of the ferrocenylethynyl fragment.

3.2. *closo*-Carborane Anions as Ligand Substituents (Alkynyl/Acetylide Ligands)

Finze and co-workers have reported some interesting coordination chemistry with alkynyl derivatives of **3** that are metalated at the C-terminus of the alkyne (acetylide), the π-bond of the alkyne, or both coordination modes simultaneously.[114] Either way, these bonding modes are distinct from the direct metalation of the C vertex of the clusters in the previous section, as the cluster is functioning as an R group attached to a ligand. A separate report of ferrocenyl alkyne derivatives of **3** has also been published[115] but is not described in detail here because the ferrocene is merely a spectator substituent, as the previous alkynyl derivatives in Scheme 10[113] show these ligands are prepared via Pd-catalyzed cross coupling.[116,117]

Finze and co-workers first reported[114] such ligands as a series of Au complexes that were synthesized in the context of self-assembly supramolecular chemistry. In this report, the B-ethynyl carborane **62** was reacted with 2 equiv of the corresponding R_3PAuCl complex in the presence of a base to form complexes **63**−**65** (Scheme 11). The reaction and bonding are rather complex in these systems where the acetylide ligand displaces chloride from R_3PAuCl to form the transient anionic species $[K]^+[R_3PAu\text{-}CC\text{-}3]^-$. $[K]^+[R_3PAu\text{-}CC\text{-}3]^-$ then undergoes salt metathesis with R_3PAuCl, eliminating KCl, to generate the complex ion pair $[PR_3Au]^+[R_3PAu\text{-}CC\text{-}3]^-$ **63**. Here, the Au counteranion with the acetylide ligand forms a π-complex with the phosphine-supported Au counterion. It was found that **64** and **65** dimerized both in the solid state and in solution. When the phosphine ligand is large (iPr_3P), as in **63**, the species remains a monomer; however, when the phosphine is smaller (Me_3P or Et_3P), the compounds dimerize to form tertrametallic clusters held together by aurophilic interactions as in **64** and **65** (Scheme 11). The dimeric nature of **64** and **65** is retained in solution, with the latter existing in equilibrium with its monomeric form.

Subsequently, Finze and co-workers found that the same ethynyl carborane salt **62** could be utilized to make a variety of

DOI: 10.1021/acs.chemrev.8b00551
Chem. Rev. XXXX, XXX, XXX−XXX

Scheme 12. Synthesis of Ag Polymer 66 and Ag Cluster 67

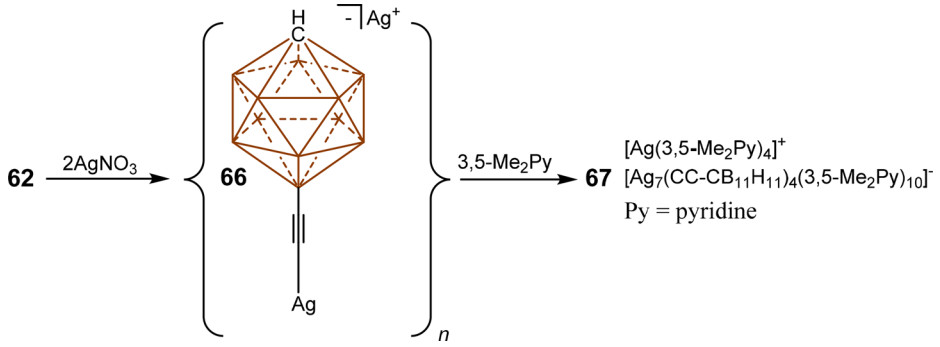

complex self-assembled structures with Ag(I).[118,119] As shown in Scheme 12, they reacted **62** with 2 equiv of $AgNO_3$ to form the polymeric **66**.

Although the exact molecular structure of **66** was not reported, it was shown to be a useful precursor for a library of complex self-assembled aggregates formed by the addition of various pyridine derivatives. These compounds, exemplified by **67**, showed exceptional phosphorescent properties for Ag(I) clusters.[119] Most recently, Finze and co-workers have reported that capping the end of the alkyne functionality with a Ph or iPr$_3$Si group allowed for the formation simpler monomeric and dimeric Ag complexes.[120]

3.3. *closo*-Carborane Anions as Ligand Substituents for Phosphines

Despite the many variations of ligands that exist, those containing *closo*-carborane anions **3** and **4** as ligand substituents are rare. In fact, aside from the π-complexed alkyne functionalities mentioned in the previous section, there are only two other types of ligands bearing *closo*-carborane anion substituents (phosphines and N-heterocyclic carbenes). While other functionalized clusters containing pendant groups with the potential to act as a ligand toward transition metals (e.g., isocyanides, nitriles, amides, etc.) have been reported, no examples in which these species function as ancillary ligands toward transition metals have yet been disclosed. There are also a few other reports, particularly by Duttwyler and co-workers, containing functionalized carborane anions as isolated intermediates in catalytic cycles.[121,122] As mentioned in the Introduction, such species fall in the category of catalytic methods for the functionalization of **3** and **4** and thus will not be discussed here. In this section, we will discuss the synthesis of anionic phosphine ligands, their coordinative properties, and their implementation in catalysis.

3.3.1. Phosphine Ligand Synthesis. As a small portion of a broader paper dealing with the synthesis of weakly coordinating anions, Reed and co-workers reported in 1993[123] the first phosphine **68** functionalized with the carborane anion **3** (Scheme 13). Subsequently, Reed reported the synthesis of the hexabrominated compound **69**.[124] In compound **69**, the bromination occurs at the lower pentagonal belt and antipodal boron (boron opposite the C vertex). Later, Finze and co-workers reported[125] the synthesis of a variety of other differentially functionalized anionic carboranyl phosphines, including **70**. However, in all cases, the ligand properties of such species with respect to transition metal chemistry and catalysis were never investigated. In an analogous reaction sequence, Lavallo and co-workers first reported the synthesis of an anionic carboranyl phosphine **71**, featuring the smaller *closo*-

Scheme 13. Synthesis of Anionic Carboranyl Phosphines

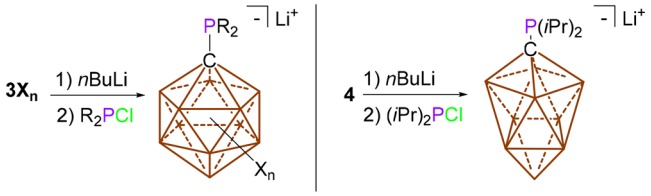

68: R= Ph, $X_n = H_{11}$
69: R = *t*Bu, $X_n = Br_6$
70: R = *i*Pr, X_n = H

71

carborane anion **4**. The latter group has launched a program to elucidate the ligand properties of such phosphines in the context of catalysis that will be discussed in the following sections.

3.3.2. Ligand Properties of Anionic Carboranyl Phosphines. The inductive effects of the C-functionalized neutral clusters $H_2C_2B_{10}H_{10}$ and $HC_2B_8H_{10}$, which are isoelectronic with **3** and **4**, were first elucidated by Holm[126] and Zhakharkin,[127] respectively. Both of these clusters are strong electron-withdrawing groups when C-functionalized, more so than a benzene ring. Spokoyny later showed that when the B vertices of $H_2C_2B_{10}H_{10}$ derivatives are covalently bound to a coordinating ligand the cluster becomes a potent electron-donating group.[13,128,129] Recently, Lavallo and co-workers reported the first study of the inductive effects of phosphines appended with C-functionalized clusters **3** and **4**.[130] This report resulted in a series of anionic Rh carbonyl complexes **72** and **73**, which are isoelectronic with well-known $[L_2Rh(CO)_2]^+$ compounds. Complexes **72** and **73** were synthesized by reacting $[(solv)_2Rh(CO)_2]^+$ cations generated in situ, with either ligand **70** or **71** (Scheme 14). By analyzing the IR stretching frequencies of **72** (2012 cm^{-1}) and **73** (1997 cm^{-1}) and comparing these data with known $[L_2RhCO_2]^+$ systems, one can conclude that unlike the neutral C-functionalized derivatives of $H_2C_2B_{10}H_{10}$ and $HC_2B_8H_{10}$, **3** and **4** are potent electron-donating groups. Cluster **4** is a stronger donor than **3** because of its higher charge density, because of its smaller size. Figure 8summarizes the inductive effects of **3** and **4** relative to *o*-carborane, a phenyl group, and an isopropyl group.

In addition to the previous study, the same group has investigated the coordinative ability of the pendant ligand substituent **3** in ligand **70**. Reaction of **70** with $(ClIrCOD)_2$ in benzene yields the unusual zwitterionic species **74** (Scheme 15).[131] In the solid state, two cage B−H units interact with the metal center in an agostic "like" manner. Weller[27−32] and Spencer[33] have reported related σ-complexes of the unfunctionalized anion **3** with Rh and Pt, respectively. The double B−H

DOI: 10.1021/acs.chemrev.8b00551
Chem. Rev. XXXX, XXX, XXX−XXX

Scheme 14. CO Stretching Frequency Analysis

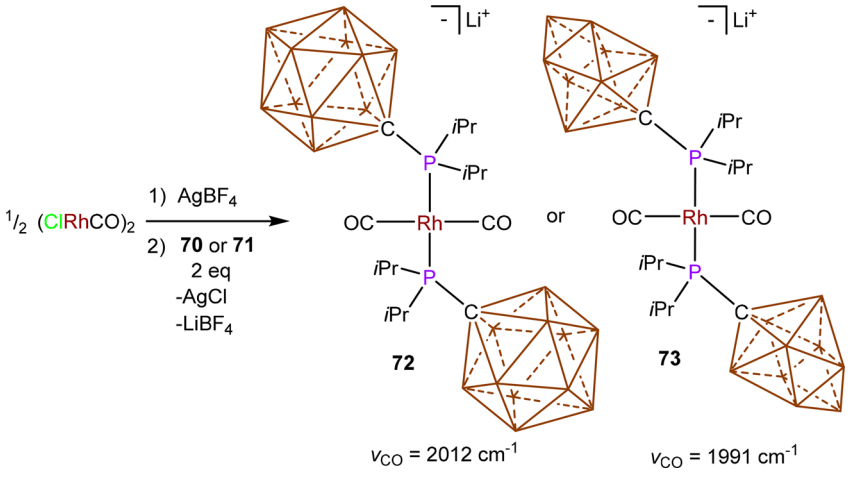

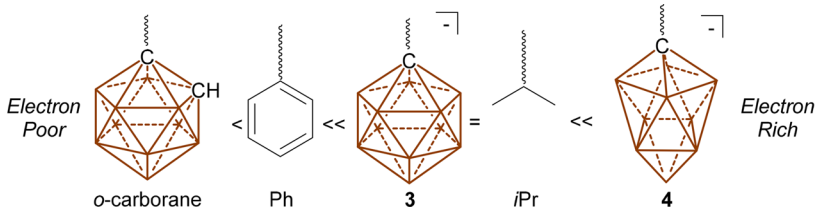

Figure 8. Increasing donor ability from left to right of the *o*-carborane, Ph, **3**, *i*Pr, and **4**.

Scheme 15. Synthesis of Ir Complex 74

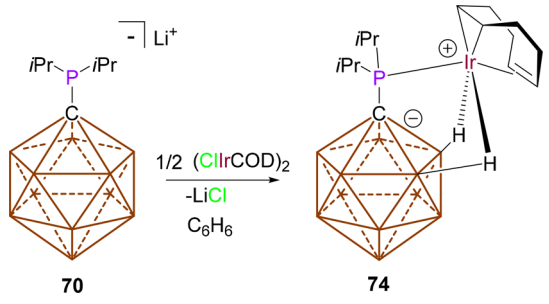

binding mode in **74** conveys an extremely weak *trans* influence to the corresponding olefinic double bond, as the "double bond" is extremely elongated [1.451(4) Å] to the point where a metallocyclopropane formalism better describes the system. This observation can be rationalized as the cluster being such a weak donor substituent that it is essentially not at all antibonding with respect to the *trans*-olefin, allowing for better d–π to π^* overlap for backbonding. Additionally, solution-based variable-temperature NMR studies were performed that showed that the carborane–P bond freely rotates at room temperature and has a rotational barrier of approximately 8 kcal/mol at −80 °C.

As mentioned in the Introduction, neutral carborane-based ligands have not displayed outstanding performance during catalysis. Evidence for this is that the neutral clusters are well-known to undergo cage degradation and facile B–H cyclometalation reactions.[14] In another study, two isoelectronic Ir(I) compounds, featuring a charged carborane substituent and a neutral carborane substituent, were targeted in an effort to investigate their different stabilities toward B–H cyclometalation.[132] First, the zwitterionic compound **74** was converted to its anionic chloride derivative by the addition of NMe_4Cl, to afford the stable Ir(I) derivative **75** (Scheme 16, left). For comparison, the isoelectronic derivative featuring a neutral carboranyl phosphine **76** was targeted (Scheme 16, right). However, the neutral isoelectronic version of **75** could not be observed; instead, a cage B–H bond instantly underwent oxidative addition to afford the octahedral Ir(III) boryl hydride **77**. This study convincingly shows that it is more difficult to B–H activate cluster **3** compared to its neutral analogue. With that

Scheme 16. Cyclometalation Resistance of 3

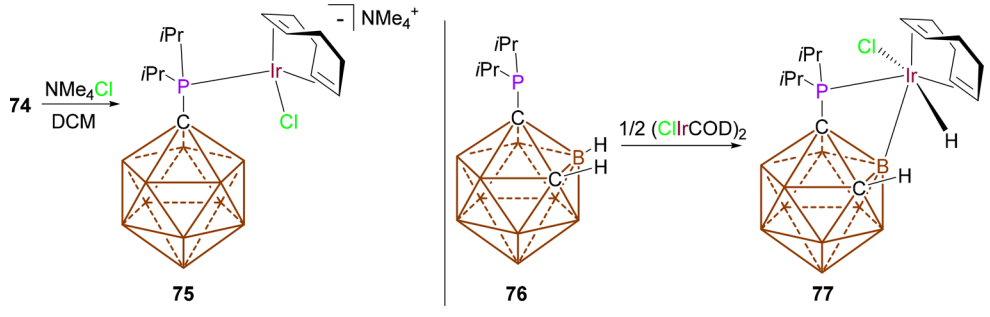

DOI: 10.1021/acs.chemrev.8b00551
Chem. Rev. XXXX, XXX, XXX–XXX

in mind, an impressive catalytic B−H functionalization methodology of **3** has been reported by Weller,[27,29] Duttwyler,[122,133] and others[11] via a cyclometalation−deprotonation instead of direct B−H oxidative addition.

3.3.3. Phosphine Ligands in Catalysis. In 2013, Lavallo and co-workers reported the first utilization of a ligand containing a *closo*-carborane substituent in catalysis.[134] Specifically, the reported synthesis of ligand **78** and the reaction with ClAuTHT formed the zwitterionic complex **79** (Scheme 17).

Scheme 17. Synthesis of Au Complex 79

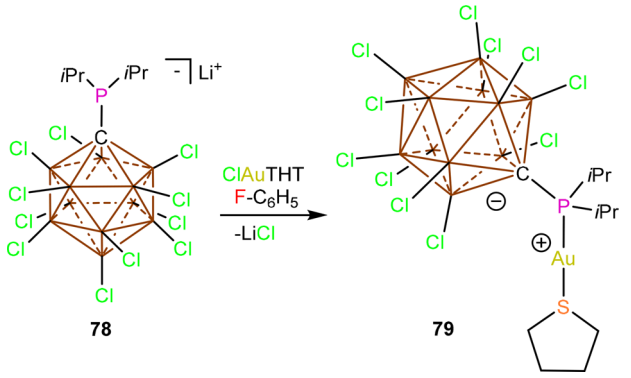

Notably, ligand **78** has a Tolman cone angle of 204°, which shows that it is much bulkier than P(*t*Bu)$_3$ (cone angle of 182°). Nearly all previous examples of Au catalysts require an acid or Ag$^+$ halide abstraction agent to generate a highly electrophilic Au$^+$ catalyst. These activators add complexity to the reaction "soup" and at times can act as catalysts themselves. In contrast, **79** is a single-component system that does not need an activator. As outlined in Table 4, catalyst **79** displays exceptional activity for certain substrates in the hydroamination of alkynes with amines. Entries 3−11 are particularly exciting as turnover numbers ranging from 22000 to 95000 are achieved, which are several orders of magnitude more active than nearly all systems for any gold-catalyzed reaction. It was hypothesized that this unprecedented activity is the result of both the single-component nature of the catalyst, which ensures rapid initiation of all catalyst molecules, and electrostatic stabilization of the Au$^+$ center by the tethered perchlorinated carborane substituent.

Subsequently, the same group reported a zwitterionic Pd allyl complex **80** (Scheme 18).[135] The solid-state structure revealed

Scheme 18. Synthesis of Zwitterionic Pd Species 80

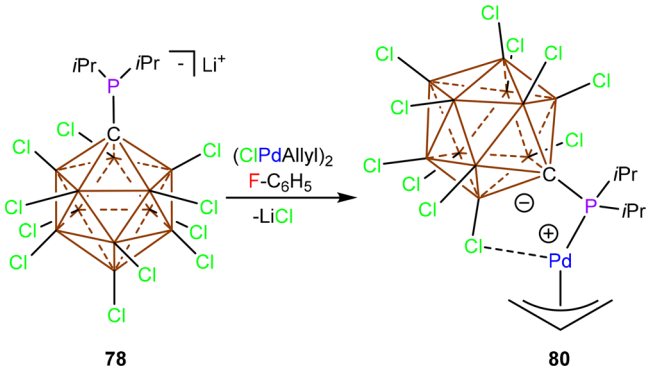

that a chloride of the carborane anion was occupying one of the coordination sites around the desired square planar palladium center. However, as revealed by ^{11}B NMR, the local C_{5v} symmetry of the carborane cluster is preserved, even when it is cooled to −90 °C, indicating free rotation of the P−C$_{cluster}$ bond. This system is reminiscent of Drent-type[136] olefin polymerization catalysts supported by anionic phosphine sulfonate ligands, and thus, its reactivity with simple olefins was investigated (Scheme 19). Unfortunately, **80** does not react with ethylene (1 atm, 80 °C, CD_2Cl_2). Furthermore, **80** rapidly

Table 4. Hydroamination of Alkynes with Primary Amines in the Presence of Catalyst 76

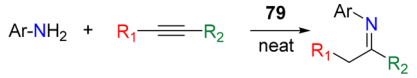

entry	Ar[a]	R$_1$	R$_2$	mol %	h	°C	% yield[b]	TON
1	Ph	H	Ph	0.1	1	25	>95	>950
2	Ph	H	Ph	0.01	16	50	>95	>9500
3	Ph	H	Ph	0.004	16	50	88	22000
4	Mes	H	Ph	0.001	24	50	67	67000
5	Dipp	H	Ph	0.001	24	50	85	85000
6	Ph	H	4-FC$_6$H$_4$	0.001	24	50	54	54000
7	Mes	H	4-FC$_6$H$_4$	0.001	24	50	75 (60)[c]	75000
8	Dipp	H	4-FC$_6$H$_4$	0.001	24	50	92	92000
9	Ph	H	4-MeOC$_6$H$_4$	0.001	24	50	90	90000
10	Mes	H	4-MeOC$_6$H$_4$	0.001	24	50	94 (93)[c]	94000
11	Dipp	H	4-MeOC$_6$H$_4$	0.001	24	50	>95 (88)[c]	>95000
12	Ph	Ph	Ph	0.1	24	80	89.5	895
13	Mes	Ph	Ph	0.1	24	80	67	670
14	Dipp	Ph	Ph	0.1	24	80	78.5	785
15	Ph	H	*n*-C$_4$H$_9$	0.2	24	80	86.5	435
16	Mes	H	*n*-C$_4$H$_9$	0.2	24	80	86	430
17	Dipp	H	*n*-C$_4$H$_9$	0.2	24	80	>95	>475

[a]Abbreviations: Dipp, 2,6-diisopropylphenyl; Mes, mesityl (2,4,6-trimethylphenyl). [b]The yields were determined by NMR spectroscopy by the direct integration of the peak for the alkyne starting material with respect to the peak for the imine product and are given as the average for two catalytic reactions. No side reactions were observed. [c]The yield of the isolated product is given in parentheses.

DOI: 10.1021/acs.chemrev.8b00551
Chem. Rev. XXXX, XXX, XXX−XXX

Scheme 19. Reactivity of 80 with Simple Olefins

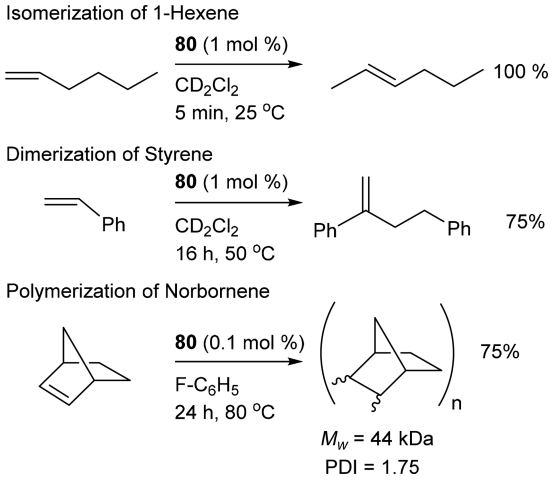

isomerizes 1-hexene to its internal isomer and dimerizes styrene at 50 °C. Upon reaction with norbornene at 80 °C, a 75% yield of polynorbornene was achieved with a polydispersity index of 1.75 and a weight-averaged molecular weight (M_w) of 44 kDa. While the catalytic performance of **80** is rather underwhelming, it still serves as a proof of principle that ligands like **78** have the possibility of being utilized in olefin polymerization catalysis. The thermal stability is also noteworthy as nearly all Pd olefin polymerization catalysts rapidly decompose at ≤70 °C.[136]

Later, the same authors reported a very unusual dianionic two-coordinate Pd(0) complex **81** (Scheme 20), which was accessed via reaction of ligand **80** with $(TMSCH_2)_2PdCOD$.[137] When dissolved in neat Cl-C_6H_5, complex **81** undergoes an exceptionally fast oxidative addition reaction at ambient temperature (9 min for quantitative oxidative addition), via the intermediate **82**, to yield **83** and **84** in a 9:1 ratio. The reaction was investigated both experimentally and computationally. The process begins by an essentially barrier-less ligand dissociation of one phosphine ligand **70** and subsequent coordination of the arene. Then a low-energy barrier, oxidative addition (4 kcal/mol) produces **82**. The intermediate **82** contains an aryl ligand as well as a phosphine **70** that is stabilized by agostic-like interactions with the B−H cage. The desirable monoanionic compound **83** forms via reassociation of **70** and simultaneously eliminates LiCl. Compound **84** arises from **82** via a divergent σ-bond metathesis of a B−H bond with the aryl ligand to produce benzene, followed by reassociation of **70**.

Comparatively, $Pd(PCy_3)_2$ affords 70% conversion in 24 h and $Pd(P(tBu)_3)_2$ shows no reactivity at ambient temperature. Buchwald has reported a few systems that display faster oxidative addition of chloro-arenes, but the species undergoing this reaction cannot be isolated.[138,139] The remarkable reactivity of **81** is thought to occur because two negatively charged phosphines bound to the zero-valent Pd center create a situation in which Coulombic repulsion renders ligand dissociation very favorable. The result is rapid access to the monophosphine-ligated Pd(0) intermediate **82**, which readily undergoes oxidative addition at ambient temperature. To highlight the difference in the electronic properties of CB_{11} substituents and isoelectronic C_2B_{10} substituents, compound **85** was prepared (Scheme 21). This neutral dicoordinate Pd(0) species does not undergo oxidative addition with Cl-C_6H_5, even at elevated temperatures.

Scheme 20. Rapid Oxidative Addition of Cl-C_6H_5

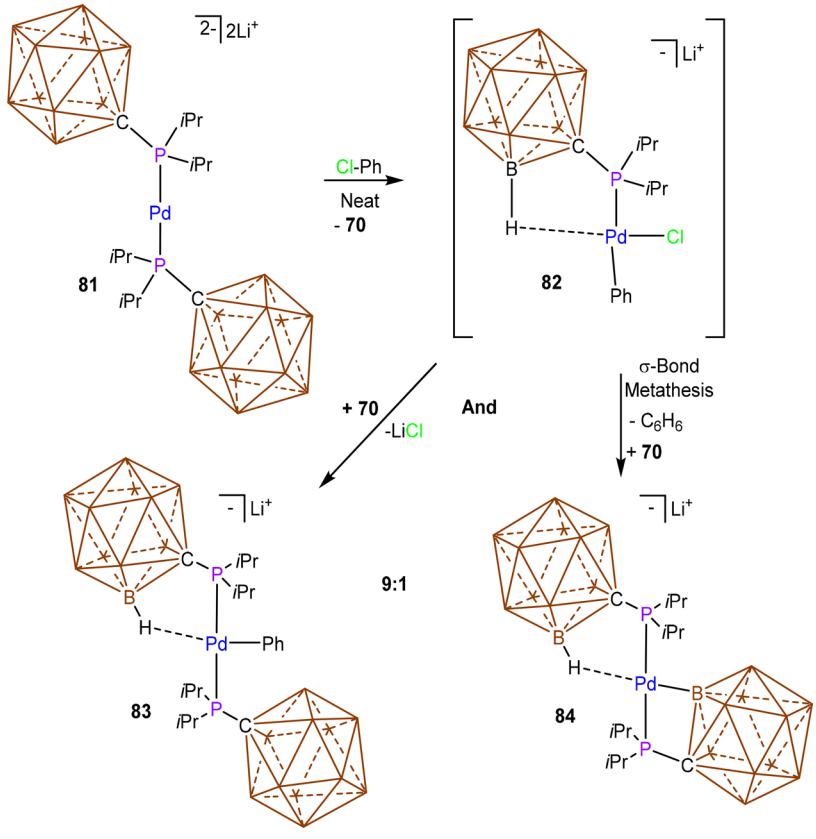

DOI: 10.1021/acs.chemrev.8b00551
Chem. Rev. XXXX, XXX, XXX−XXX

Scheme 21. Compound 85, Which Is Isoelectronic and Steric with 81 and Does Not React with Cl-C_6H_5

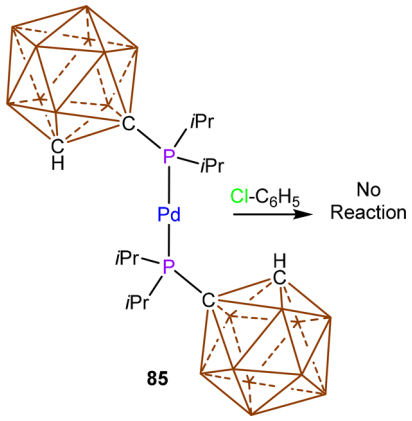

Compound **81** is also a competent catalyst for the Kumada coupling with simple chloro-arenes, but the activity of the catalyst is nowhere near the best catalyst for the same reaction. The lower activity, relative to that of fast oxidative addition, is likely the result of slow transmetalation/reductive elimination steps or simply catalyst deactivation via similar σ-bond metathesis pathways that form **84**. The utilization of B−H functionalized cluster substituents that prevent cyclometalation may result in more active catalysts.

3.4. N-Heterocyclic Carbene Ligands with Anionic Carborane Substituents

Recently, Lavallo and co-workers have designed the synthetic methodology to access several classes of NHCs that contain carborane clusters directly bound to the nitrogen atom of the NHC ring.[140−142] This section highlights the synthesis and unique behavior of these species as well as the preliminary coordination chemistry of these ligands with Au. Although no catalysis has yet been reported with these systems, it seems likely such ligands will find utility given the success with the phosphines in the previous section.

Although anionic amino carboranes, such as **86**, have been known for decades, there has been little to no exploration of their simple condensation chemistry with aldehydes or ketones (Scheme 22).[140−142] The pK_a of **86** has been determined experimentally to be 6.0 and is slightly higher than that of aniline, which is 4.6.[143] As illustrated in Scheme 22, **86** behaves like a typical aliphatic or aryl amine, which allows access to the dianionic diamine, **87**, and monoanionic imidazolium salt, **88**.[142] While the use of **87** as a ligand has not been reported, the ensuing imidazolium anion **88** can be converted to an NHC.

Depending on the conditions and base employed, the imidazolium anion **88** is a suitable precursor to three unique NHC lithium salts, **89**−**91** (Scheme 23). Selective C-2 deprotonation of **88** can be achieved using lithium bis(trimethylsilyl)amide (LiHMDS) to afford the so-called "normal" carbene **89**. Selective C-5 deprotonation to form the "abnormal" NHC[144] **90** is accomplished by using lithium diisopropylamide (LDA) at −78 °C. NHCs **89** and **90** are the first examples of two NHC constitutional isomers that also have the ability to form two different NHC isomers from a single precursor. The energy of the abnormal C-5 isomer **90** is higher than that of **89**, and **90** slowly isomerizes to the normal C-2 species over time. Imidazolium anion **88** can also be doubly deprotonated[145] with *n*-BuLi to form the trianionic C-2/C-5 lithium salt **91**. The selective formation of three different NHCs from a single precursor is not possible with standard hydrocarbon substituents and is likely the result of both electronic and steric effects conveyed by the carborane groups.

Scheme 23. Bis(Carboranyl) NHC Li Salts

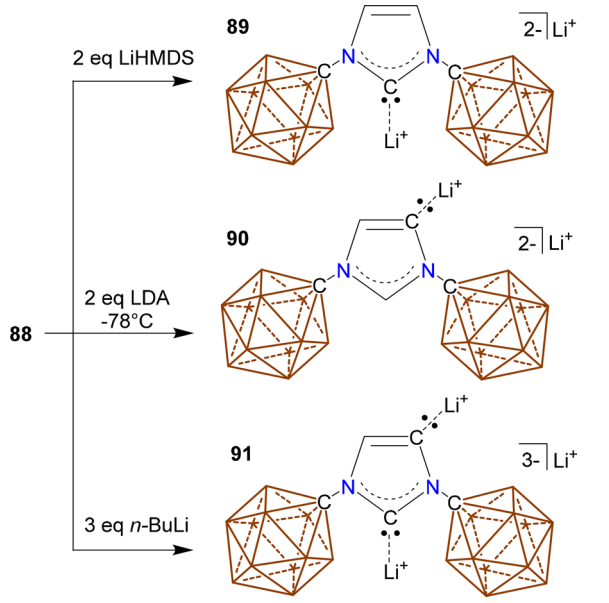

Subsequently, the synthesis of an unsymmetrical NHC featuring only one carborane substituent was reported.[141] This compound was produced from the reaction of amine **86** with oxyzolium cation **92**, affording the zwitterionic imidazolium species **93** (Scheme 24). Compound **93** reacts with LiHMDS to cleanly afford the "normal" monoanionic C-2 NHC isomer **94**, but all attempts to selectively prepare the abnormal C-5 isomer failed. However, double deprotonation to form the dianionic species **95** could be achieved with *n*-BuLi (Scheme 25). Interestingly, the presence of the carborane substituent induces selective formation of the isomer with the NHC backbone lone pair closest to the mesityl ring. This effect is likely the result of a

Scheme 22. Condensation Chemistry with Amine 86

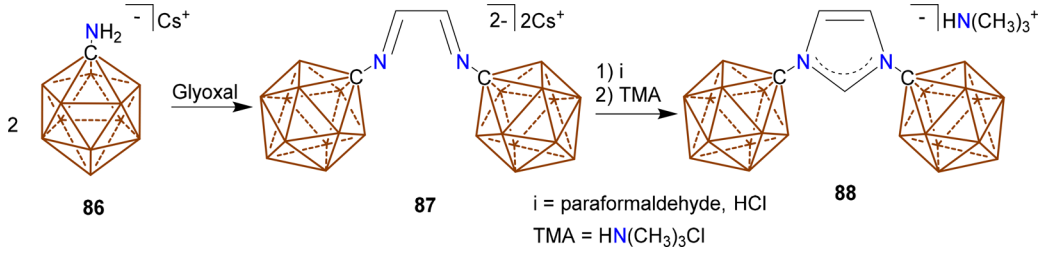

DOI: 10.1021/acs.chemrev.8b00551
Chem. Rev. XXXX, XXX, XXX−XXX

Scheme 24. Synthesis of Unsymmetrical Imidazolium Species 93

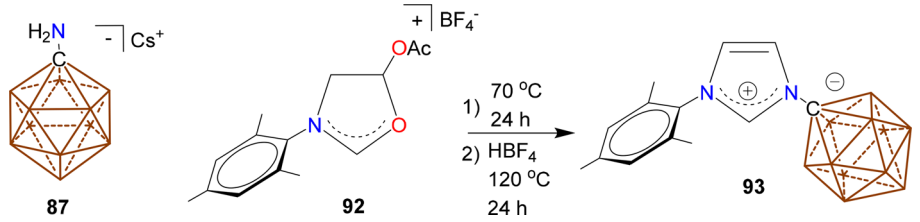

Scheme 25. Synthesis of Unsymmetrical NHC Li Salts

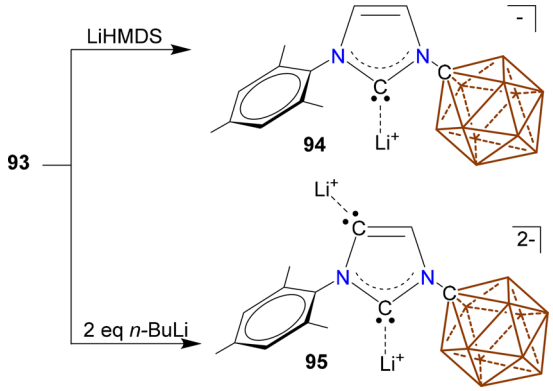

combination of electrostatic repulsion and steric pressure from the large carborane cluster.

Most recently, a new class of unsymmetrical NHCs featuring dianionic carborane clusters (dicarbollide ions) were prepared in a similar fashion (Scheme 26).[140] Although they are not *closo*-carborane anions, we include the dicarbollide[146] substituted NHC here given its similarity to the previously mentioned carbenes. The zwitterionic imidazolium **96** can be accessed in a fashion analogous to that used for **93**. In this case, the bridging hydride H_a is more acidic than the imidazolium C−H_b; thus, it can sequentially be deprotonated first to form the anionic imidazolium dicarbollide **97**, which adopts a sandwich structure, and then subsequently deprotonated to form the carbollide NHC **98**.The dicarbollide ions are cyclopentadienyl mimics,[146] and thus, this class of ligands should provide unique transition metal complexes and perhaps catalysts in the future, as well.

3.4.1. Au Complexes Di- and Mono-Carboranyl-Substituted NHCs 89 and 94. So far, the only reported transition metal complexes of anionic carboranyl NHCs consist of adducts of **89** and **94** with Au(I).[147] Reaction of **89** with Cl-Au-S$(CH_3)_2$ in fluorobenzene produces the anionic Au(I) complex **99**. There is a side reaction giving a dianionic chloride adduct, but this can easily be converted to **99** via treatment with SMe_2 in CH_2Cl_2. The analogous reaction with **94** cleanly affords the zwitterionic Au(I) species **100** (Scheme 27).

Scheme 27. Synthesis of the First Transition Metal Carboranyl NHC Complexes

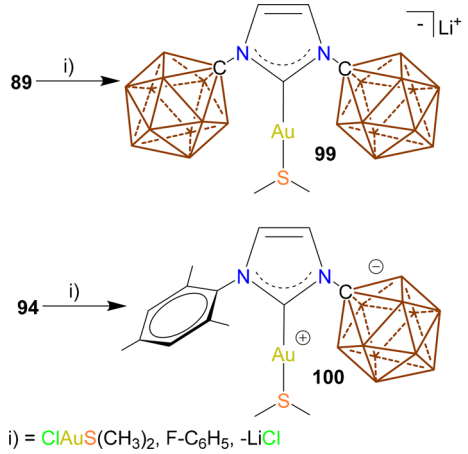

In the solid state, the NHC−Au−S angle of **96** is nearly linear at 179.7° while **100** is modestly distorted form linearity (171.7°). This distortion is likely caused by the steric repulsion of the carborane anion overriding the electrostatic attraction; this is further exacerbated by cation−π interaction between the Au^+ and the mesityl ring. Percent buried volume ($\%V_{bur}$) calculations[148] indicate that replacement of an adamantyl group by a hydride-substituted icosahedral carborane anion results in a 3.7% increase in $\%V_{bur}$. The catalytic activities of **99** and **100** have not yet been reported.

Scheme 26. Synthesis of an NHC Featuring a Dicarbollide Ion Substituent

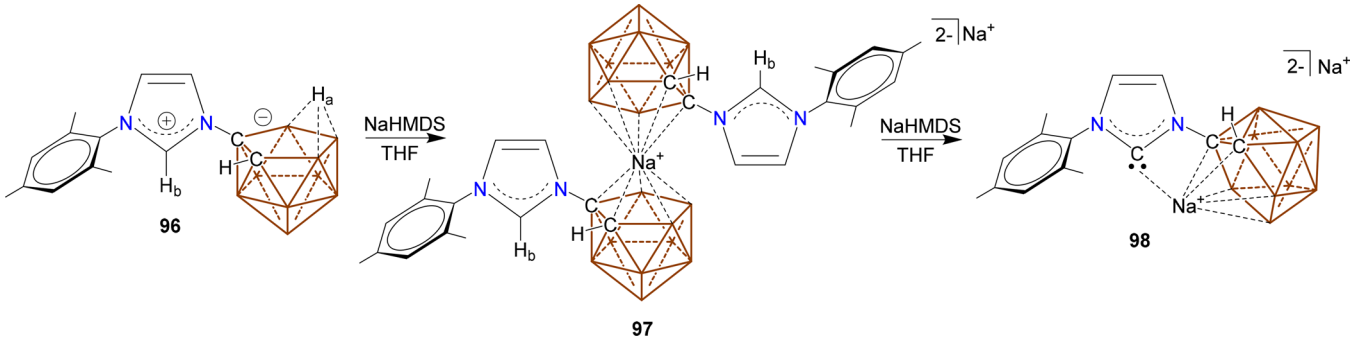

DOI: 10.1021/acs.chemrev.8b00551
Chem. Rev. XXXX, XXX, XXX−XXX

Scheme 28. Anionic Carboranyl Radicals

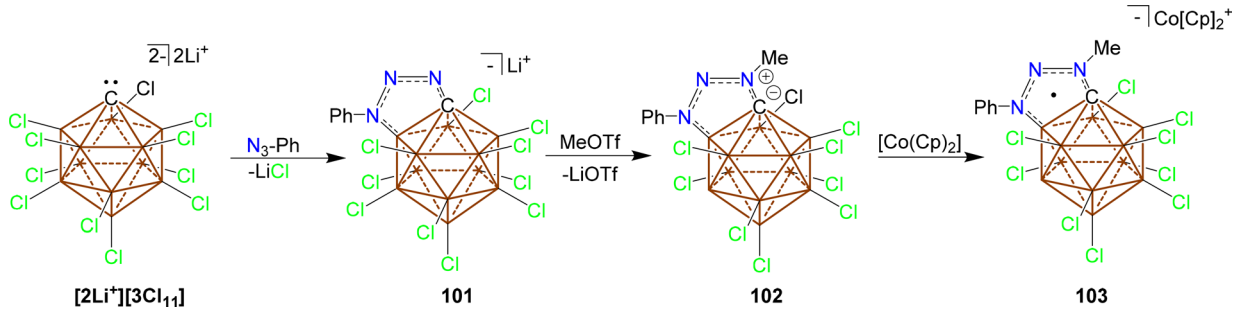

4. *CLOSO*-CARBORANE ANIONS AS SUBSTITUENTS TO STABILIZE RADICALS

Michl has isolated some neutral carborane radicals and electrochemically characterized other radicals derived from **3**, where the unpaired electron is delocalized throughout the cluster core.[15] The purpose of this section is to highlight the nonclassical potential of derivatized **3** to stabilize radicals outside of the cluster framework.

Triazole radical anions eluded isolation for many decades until a carborane-substituted derivative provided ready access to this interesting family of reactive compounds (Scheme 28).[149] A novel "click-like" reaction between $[\mathbf{Li}^+][\mathbf{3Cl}_{11}]$ and azides Ph-N_3 was discovered to access triazole **101**,[150,151] which possesses aromatic characteristics inside and outside the cluster core (Scheme 28). Notably, these reactions were demonstrated to be effective for various azides (for N_3-R, R = Ph, 4-FC_6H_4, 4-$MeOC_6H_4$, 2-MeC_6H_4, or Ad).[150] Cyclic voltammetry (CV) of **101** revealed that irreversible reduction occurs at high negative potentials and no observable oxidation. To decrease the high negative potential associated with the radical dianion, the authors formed a zwitterionic species **102**, via methylation of **101**. Electrochemical analysis of **102** showed a reversible reduction at −0.87 V versus Fc/Fc^+ and irreversible reduction above −2.5 V (Fc/Fc^+). Utilizing this information, the authors chose cobaltocene (reduction potential of −1.33 V vs Fc/Fc^+) as a reducing agent to form an isolable radical anion **103**. Unlike **102**, **103** shows no sign of extended conjugation between the three-dimensional cluster core and two-dimensional triazole π-system (Scheme 28). The spin density is completely localized outside of the cluster on the three triazole nitrogen atoms with the carborane cluster functioning as a spectator.

5. *CLOSO*-CARBORANE ANIONS FOR ENERGY STORAGE APPLICATIONS

Given the enormous electrochemical stability of *closo*-borohydride **1**, **2**, and *closo*-carborane anions **3** and **4**, they should be ideally suited for electrolyte applications in batteries.[152] Indeed, salts based on **1** and **2** were explored as solution-based electrolytes for Li-ion batteries as early as the 1970s. For example, primary liquid cathode $Li/SOCl_2$ cells, which utilized $2[Li]^+[B_{10}Cl_{10}]^{2-}$ and $2[Li]^+[B_{12}Cl_{12}]^{2-}$ salts as electrolytes, were reported in 1979.[153] In 1980, Johnson and Whittingham used these same electrolytes for Exxon's work on Li/TiS2 cells. More recently, fluorinated all-boron cluster $2[Li]^+[B_{10}F_{10}]^{2-}$ and $2[Li]^+[B_{12}F_{12}]^{2-}$ salts were developed by Air Products under the label "Stabilife fluorinated electrolyte salts". The solution conductivity of these electrolytes is lower than for comparable electrolytes with $[Li]^+[PF_6]^-$, but the electrolyte solvent/salt formulation can be tuned to obtain promising cell cycling performance, especially at an elevated temperature (60 °C). The low conductivity of these materials can be explained by their inherent dinegative charge. The high electrochemical stability of these anions has been shown to provide overcharge protection for +4 V Li-ion batteries, shown with MCMB/spinel cells.

Investigations into the use of *closo*-carborane anions **3** and **4** as electrolytes are relatively new. As recently as 2015, carborane anions have attained value as weakly coordinating anions in both solution[154] and solid-state-ion conducting media[155] for the purpose of enabling advanced energy storage technologies. Their utility arises not only from their weakly coordinating properties, resulting in more conductive cations, but also from their extreme thermal, chemical, and oxidative stability.[15,20] Knapp and Boeré have elegantly determined the oxidative stability windows for several derivatives of **3**, showing that the parent compound **3** is oxidatively stable up to around 6.0 V versus Li.[152] In addition, **3** cannot be chemically reduced by any element, including Li metal.[15] *closo*-Carborane salts of **3** and **4** have found particular utility as electrolytes for solution-based Mg batteries.[154,156−160] Mg batteries are of great interest, because they are potentially safer, more cost-effective, earth abundant, and more energy dense than current state-of-the-art Li-ion batteries.[161−168] In addition, anions **3** and **4** have demonstrated high solid-state ionic conductivity of monovalent ions such as sodium and lithium near room temperature.[155,169−173] Such performance suggests anions **3** and **4** may function well as solid-state electrolytes to enable next-generation solid-state batteries.[174−178] In this section, we review the development of ion-conducting materials based on carborane anions **3** and **4** from their discovery to subsequent research progress.

5.1. Solution-Based Electrolytes for Mg Batteries

Metal salts capable of reversible oxidation/reduction reactions, while remaining electrochemically stable, are desired as electrolytes in many commercial energy storage devices. Achieving high Coulombic efficiency, retaining consistent electrochemical behavior upon repeated cycling, and remaining oxidatively stable at very positive potentials are basic considerations for materials that are excellent electrolyte candidates. While electrolyte formulations designed to facilitate lithium-ion battery chemistry are well-studied, electrolytes capable of enabling multivalent-ion battery systems remain highly desired.[165] In particular, Mg batteries stand to improve upon lithium batteries in a number of ways, including higher volumetric capacities (3833 mA h cm^{-3}), a higher gravimetric energy density compared to that of Li-graphite anodes, a significantly lower cost in anode materials, and a tendency not to form dendrites that plague electrochemical cells utilizing

DOI: 10.1021/acs.chemrev.8b00551
Chem. Rev. XXXX, XXX, XXX−XXX

metallic Li anodes.[162−167] As a result, these batteries are attractive as grid-level energy storage devices as well as compact batteries for electric vehicles and portable devices. Despite these advantages, efforts to develop these electrolytes usually result in one or multiple issues, including (1) large overpotentials associated with oxidation and reduction, (2) low redox stability, (3) low Coulombic efficiency and cycling stability, and (4) the presence of corrosive halides. Additionally, unlike Li-ion cells that function perfectly fine with a surface electrolyte interface layer (corrosion layer) at the anode surface, divalent Mg^{2+} ions cannot penetrate such barriers for Coulombic reasons. Thus, unlike Li-ion cells, Mg cells need to utilize electrolytes that do not at all react with the anode. Such issues typically lead to significantly reduced battery capacity, strict limitations on cathode selection and cell voltage, or corrosion of active materials and battery components. Thus, there is a desire for electrolytes that address all of these shortcomings in an effort to realize a magnesium battery of commercial value.

Numerous anionic organohaloaluminate species, boron-based counteranions, and weakly coordinating anions have been developed as magnesium electrolyte candidates to enable such a magnesium battery. Recently, carborane anions have gained attention as counteranions to Mg^{2+} that facilitate high performance in batteries containing a magnesium metal anode.[154,156−159] In 2015, Mohtadi and co-workers of the Toyota Research Institute published the first halide-free anionic *closo*-carborane electrolyte, [**Mg**$^{2+}$]**3**, which functions as an enabling ion conductor for magnesium batteries (Scheme 29).[154] The synthesis of [**Mg**$^{2+}$]**3** was achieved through the

Scheme 29. Mohtadi's Synthesis of [Mg^{+2}]3

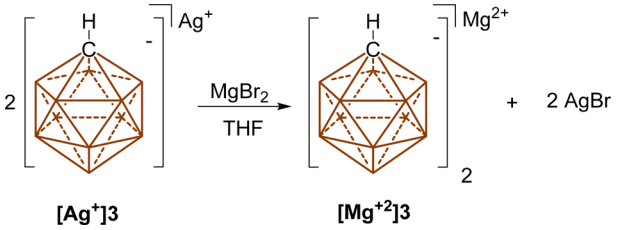

salt metathesis of commercially unavailable [**Ag**$^{+}$]**3** and $MgBr_2$ (Scheme 29). Although this route is effective, the electrolyte produced is extremely difficult to purify as trace amounts of Mg halide and Ag salts contaminate the material. This electrolyte was characterized by a very low overpotential (<250 mV vs $Mg^{0/2+}$) upon oxidation and reduction (stripping and deposition), demonstrated a high Coulombic efficiency and cycling stability (>99.5% over 100 cycles), and was anodically stable up to the oxidation of tetraglyme at 3.8 V (Figure 9). Cyclic voltammograms of [**Mg**$^{2+}$]**3** dissolved in lower-glyme solvents such as diglyme or dimethoxyethane (DME) are not pictured, as [**Mg**$^{2+}$]**3** remains insoluble or tends to crystallize out of these solvents at ambient temperatures. The low overpotential associated with [**Mg**$^{2+}$]**3** is likely due to the weakly coordinating properties of the carborane and, thus, development of a solvent-separated ion pair that results in a less obstructed magnesium cation. This separated ion pair perhaps further explains the electrochemical performance of [**Mg**$^{2+}$]**3** in contrast to coordinative MgR_2 species that tend to be ionic insulators. Likewise, the resistance of this material to oxidation is a testament to the stability of the carborane cluster (+2.35 V vs $Fc^{0/+}$) as investigated by Boeré and Knapp. The electrolyte

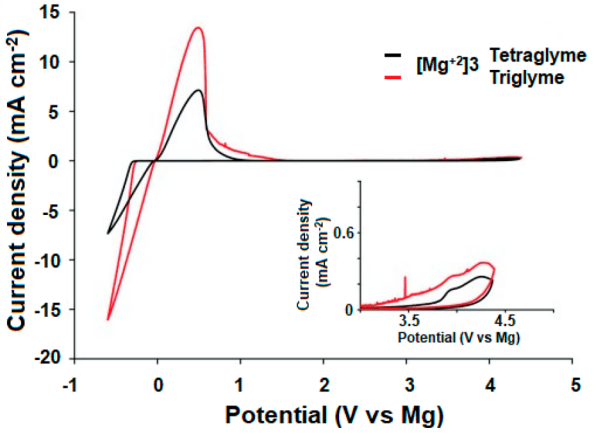

Figure 9. Cyclic voltammograms of a 0.75 M solution of [**Mg**$^{2+}$]**3** in tetraglyme and triglyme solvents. The inset shows the 3.0−5.0 V range displaying the anodic stability of both electrolytes.

[**Mg**$^{2+}$]**3** dissolved in tetraglyme displayed a significantly higher Coulombic efficiency (94.4% vs 79.6%) and was found to have a maximum conductivity in tetraglyme of 1.8 mS cm^{-1} as a 0.75 M solution. Furthermore, [**Mg**$^{2+}$]**3** contains no halides typically found in corrosive electrolyte solutions. In a testament to the noncorrosive properties and oxidative stability of [**Mg**$^{2+}$]**3**, chronoamperometric experiments with this electrolyte held at 3.0 and 3.5 V displayed only minute indications of corrosion. In the same experiment, no pitting was observed on the stainless steel electrode surface, confirming the [**Mg**$^{2+}$]**3** solutions would be compatible in stainless steel coin cells.

At the same time as Mohtadi's report of [**Mg**$^{2+}$]**3**, Lavallo and Guo developed a far more efficient synthesis of [**Mg**$^{2+}$]**3** as well as a carboranyl electrolyte with enhanced conductivity.[158] The so-called "cation reduction" method utilizes elemental Mg and the [$HNMe_3^+$] salt of **3** to produce [**Mg**$^{2+}$]**3**, resulting in only gaseous H_2 and NMe_3 as a byproducts (Scheme 30). This method decreases the expense of scale-up by avoiding precious metal byproducts (AgBr) and results in material of superior purity. Indeed, Mohtadi and other researchers at the Toyota Research Institute have abandoned[133] their initial synthetic protocol and adopted Lavallo and Guo's cation reduction methodology. In an effort to improve upon the conductivity and solubility properties of [**Mg**$^{2+}$]**3**, the authors synthesized [**MgPh**$^{+}$]**3** via comproportionation of [**Mg**$^{2+}$]**3** with $MgPh_2$ (Scheme 30). In contrast to [**Mg**$^{2+}$]**3**, [**MgPh**$^{+}$]**3** benefits from reduced positive charge rendering the Mg ion more mobile. As a result, [**MgPh**$^{+}$]**3** remains dissolved in a solution of DME at room temperature, in contrast to [**Mg**$^{2+}$]**3** that is not soluble. A 0.40 M solution of [**MgPh**$^{+}$]**3** in DME achieved a conductivity of 1.24×10^{-2} S cm^{-1}, 4 times greater than that of [**Mg**$^{2+}$]**3** in tetraglyme, successfully improving upon [**Mg**$^{2+}$]**3**. Despite the change in the coordination environment of the magnesium center to be appended with a phenyl ligand, metallic magnesium deposits were identified on the Pt^0 working electrode surface by scanning electron microscopy and X-ray diffraction studies (Figure 10). These experiments not only confirm the deposition of pure magnesium on reduction but also demonstrate, despite the added phenyl appendage of **3**[**MgPh**$^{+}$], only pure magnesium deposits are present. **3**[**MgPh**$^{+}$] reached an unprecedented oxidative stability of >4.6 V versus $Mg^{0/2+}$ on both Pt^0 and glassy carbon working electrodes (Figure 11), the most oxidatively stable magnesium electrolyte to date. Despite the change in the design motif, these results point to carborane

DOI: 10.1021/acs.chemrev.8b00551
Chem. Rev. XXXX, XXX, XXX−XXX

Scheme 30. Cation Reduction and Comproportionation To Form [Mg^{+2}]3 and [MgPh^{+}]3

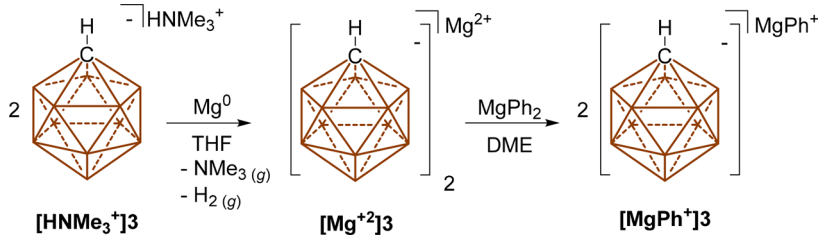

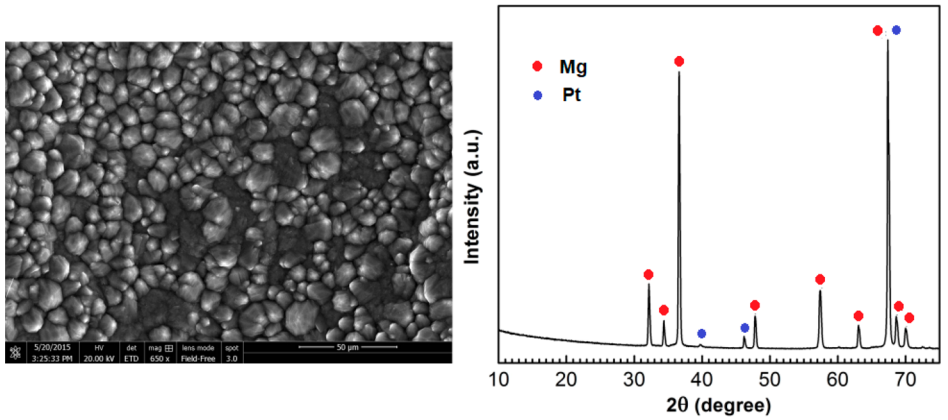

Figure 10. Scanning electron microscopy image of Mg^{0} deposits on a Pt^{0} electrode with [**MgPh^{+}**]**3** (left). X-ray diffraction of the same electrode shows the presence of only Mg^{0} and Pt^{0} species (right).

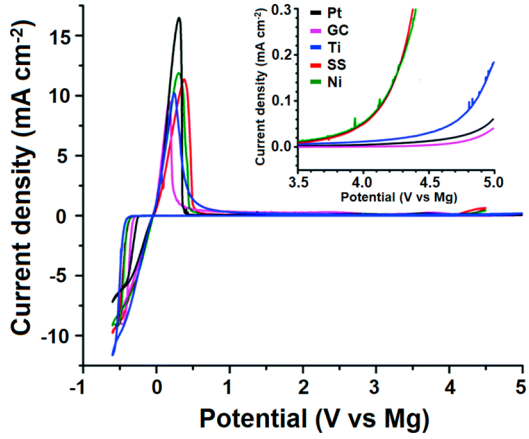

Figure 11. Cyclic voltammograms of [**MgPh^{+}**]**3** in a DME solvent against platinum (Pt), glassy carbon (GC), titanium (Ti), stainless steel (SS), and nickel (Ni) working electrodes. The inset shows the 3.5−5.0 V range displaying the anodic stability of [**MgPh^{+}**]**3**.

anions as versatile materials in the design of new electrolytes for next-generation batteries. Furthermore, the advent of carboranyl magnesium electrolytes capable of oxidative stability up to 4.6 V opens the door for exploration of novel higher-voltage cathode materials.

Subsequently, Lavallo and Guo sought to explore the less recognized **4** as a viable alternative to previously published works. Compound **4** is similar to **3** in its thermal and oxidative stability and was reported by Hawthorne to resist oxidation up to 4.56 V versus Mg$^{0/2+}$.[179] Additionally, **4** has the distinct advantage of a more economically favorable synthesis that, in contrast to **3**, does not involve the evolution of cyanide gas or employ pyrophoric sodium metal. As such, **4** was investigated in a similar manner, exploiting the [**HNMe$_3^+$**]**4** salt as a means of affording an efficient synthetic route (Scheme 31).[157]

Scheme 31. Magnesium Reduction of [HNMe$_3^+$]4 to [Mg^{+2}]4

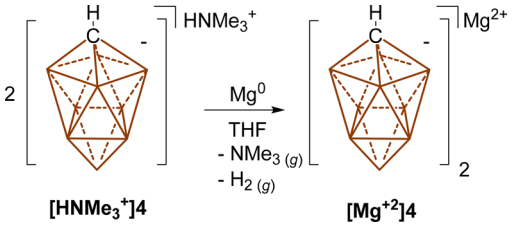

As with **3**, [**Mg^{2+}**]**4** was found to be restricted to glyme solvents due to the solubility properties of the material as well as compatibility with the magnesium metal anode. Impedance measurements of the conductivity of [**Mg^{2+}**]**4** suggested an optimum concentration of 0.45 M in tetraglyme at 1.57 mS cm^{-1}, an ionic conductivity comparable to that of a 0.75 M solution of [**Mg^{2+}**]**3** in the same solvent. When placed in a fully assembled cell consisting of a Mg metal anode and a Chevrel phase Mo_6S_8 cathode, [**Mg^{2+}**]**4** achieved an initial discharge capacity of 94 mA h g^{-1} followed by 45 mA h g^{-1} in the second cycle, followed by a steady capacity decline in subsequent cycles. While there is a striking difference in electrochemical performance between [**Mg^{2+}**]**3** and [**Mg^{2+}**]**4**, this performance is specific to pairing the electrolyte with a Mo_6S_8 cathode, and thus, other cathode materials may behave differently.

Much remains to be learned about the electrochemical behavior of anions **3** and **4** within the context of energy storage. Of current interest is the interfacial chemistry between [**Mg^{2+}**]**3** and the magnesium metal anode. In contrast to previous reports of the solid electrolyte interphase (SEI) layer with other electrolytes formed on magnesium, one study speculates that a

DOI: 10.1021/acs.chemrev.8b00551
Chem. Rev. XXXX, XXX, XXX−XXX

magnesium metal anode may function despite the development of a SEI layer from [**Mg**$^{2+}$]**3**.[133] In addition, unlike typical electrolyte anions (OTf^-, PF_6^-, BF_4^-, etc.), the carborane anions can be essentially infinitely tuned by surface substitution at the B and C vertices. Hence, a variety of functionalized carborane species displaying enhanced solubility, conductivity, and electrochemical stability likely exist. These carborane-based electrolytes are the first set of ion conductors that can reliably be used to explore novel high-capacity/voltage cathode materials, which may lead to sustainable secondary batteries with energy storage capabilities beyond those of Li-ion cells.

5.2. *closo*-Carborane Anions as Solid-State Electrolytes

Another exciting area of energy storage research focuses on the design of solid electrolytes to enable all-solid-state batteries.[174−178] Solid-state energy storage promises higher oxidative stability as well as increased gravimetric and volumetric energy density by removal of cumbersome liquid electrolyte solvents. Additionally, lack of a flammable organic solvent in contact with reactive anode materials, such as lithium or sodium metal, would alleviate many safety concerns associated with current liquid electrolytes. Thus, solid-state ion-conducting media that rival the performance of liquid electrolytes have been urgently sought.

One major problem with solid-state systems is their inability to achieve a conductivity similar to those of liquid electrolytes. In contrast to liquid electrolytes, which regularly conduct ions on the order of 10^{-2} to 10 S cm^{-1}, solid-state ion conductors tend to conduct several orders of magnitude slower. This drastic decline in ionic conductivity is primarily due to the lack of a liquid medium in which there is minimal resistance to the translational motion of ions. In the solid state, ions must navigate through a crystal lattice or glassy matrix[178] where steric interactions and Coulombic forces dictate the diffusive properties and energy landscape of the material. Typically, elevated temperatures are required to achieve an ionic conductivity comparable to those of the most successful solution-based electrolytes.

An emerging class of materials called superionic conductors (SICs) are materials that conduct above 10^{-3} S cm^{-1}, making them competitive with liquid electrolytes.[177,180] SIC behavior results from the fast migration of cations through vacancies in the crystal lattice. Migration of cations to vacancies in SIC materials tends to have low energy barriers associated with their motion, typically below 0.3 eV. These low energy barriers tend to dictate ion conductivity in SIC materials. The positions of the anions are preserved while cations become more disordered within the lattice. The anion sublattice is therefore thought to be the main factor in these low activation energies and higher conductivities. As a result, there has been significant effort spent to develop an anion sublattice capable of conducting ions quickly, efficiently, and, ideally, at near-ambient temperatures in the solid state. *closo*-Borohydrides[181−184] and carboranes[155,169−173] **1**−**4** have displayed excellent solid-state ionic conductivity, particularly **3** and **4**. Additionally, the electrochemical stabilities of *closo*-borohydrides, carboranes, and other notable derivatives have recently been reviewed, many displaying an anodic stability greater than those of common solvents used in liquid electrolytes.[154,157,158,185] This section will highlight the recent progress with **3** and **4** as SICs.

Anhydrous versions of sodium or lithium salts of **1**−**4** are essential for achieving high ionic conductivities in these materials.[155,170] Anhydrous salts ensure that the cations in the lattice are free of coordinating solvents, allowing them to migrate more easily. However, these alkali salts are incredibly hygroscopic, and coordinated solvents are generally present after the process of salt metathesis. To remove all coordinated solvent, these materials were heated above 400 K under vacuum for several hours to days and then handled under an inert atmosphere to ensure no recoordination of the solvent. Only then can these materials be pressed into stand-alone electrolyte/separators, approximately 1.5−3 mm thick, which can then be tested for their conductive properties.

In 2014, Udovic and co-workers began investigating the sodium and lithium salts of the isostructural, isoelectronic, dianionic *closo*-dodecaborate (**1**) and decaborate (**2**) clusters as possible solid-state ion-conducting materials (Figure 12).[183,184]

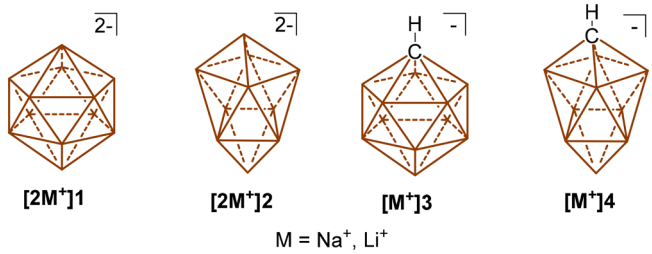

Figure 12. *closo*-Dodecaborate ion pair, [2**M**$^+$]**1**, and *closo*-decaborate ion pair, [2**M**$^+$]**2**. Unlabeled vertices = B−H; M = Na^+ or Li^+.

The SIC behavior of [2**Na**$^+$]**1** and [2**Na**$^+$]**2** was observed after thermally induced phase transitions at 529 and 360 K, respectively. The analogous lithium salts [2**Li**$^+$]**1** and [2**Li**$^+$]**2** achieved similar conductivities only at temperatures of >600 K.

While these materials had very high transition temperatures, a hysteresis in the SIC transition temperatures was observed. Hysteresis refers to how a material's history, in this case thermal history, will affect a compound's present properties. These order−disorder, hysteretic phase changes are well-known for many solid electrolyte systems[186] and allow the SIC phases of [2**Na**$^+$]**1** and [2**Na**$^+$]**2** to remain stable at temperatures lower than the phase transition temperature. This hysteresis allows many of the SIC phases of **1** and **2** [also **3** and **4** (vide infra)] to remain stabilized at lower temperatures by heating the material before use.

In 2015, Udovic and co-workers observed the SIC behavior of Li^+ and Na^+ salts of **3**.[155] The [**Li**$^+$]**3** and [**Na**$^+$]**3** salts conduct at 0.15 and 0.12 S cm^{-1}, above their transition temperatures of 395 and 380 K, respectively. These materials underwent the transition back to their much less conductive phases at 383 and 354 K, respectively. Figure 13 shows the ionic conductivity of these materials after their initial heating cycles into the SIC phase. Both [**Li**$^+$]**3** and [**Na**$^+$]**3** had energies of activation of 0.22 eV in their SIC phases, making them competitive with other SIC materials (e.g., Na_3PSe_4 and $Li_{10}GeP_2S_{12}$) (Figure 13).[174] In addition, these carborane conductors are compatible with metallic Li and Na whereas traditional conductors like Na_3PSe_4 and $Li_{10}GeP_2S_{12}$ are not. The alkali metal salts **3** outperformed both **1** and **2**, with lower SIC transition temperatures, lower energies of activation, and higher conductivities. Despite the improved performance of these materials, SIC phases were unstable at room temperature, making them unsuitable for most energy storage applications. A battery containing a 50 wt % mixture of TiS_2 and [**Li**$^+$]**3** as a cathode material, [**Li**$^+$]**3** solid electrolyte, and a lithium anode was constructed. The battery operated at 403 K and was cycled five times at 0.2 C. The battery had an approximate discharge

DOI: 10.1021/acs.chemrev.8b00551
Chem. Rev. XXXX, XXX, XXX−XXX

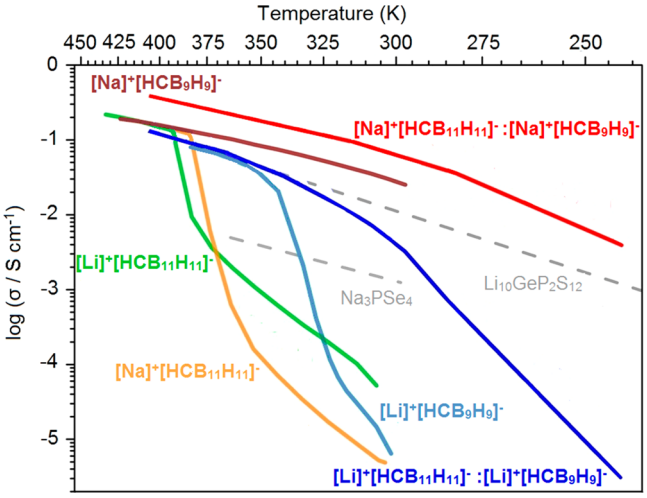

Figure 13. Temperature dependence of the ionic conductivity (σ) of all studied carborane anions and some common lithium SICs.

capacity of 175 mA h g^{-1} with a 95% Coulombic efficiency after the third cycle. This was considered a proof of concept for the incorporation of these materials into batteries.

The search for a material with a high ionic conductivity in the solid state led to the investigation of alkali metal salts of **4**.[170] The SIC behavior was observed at even lower temperatures for [Li^+]**4** and [Na^+]**4** compared to [Li^+]**3** and [Na^+]**3**. The lithium and sodium salts underwent transitions into SIC phases at 353 and 310 K (Figure 13) with energies of activation of 0.29 and 0.20 eV, respectively. An undesirable hysteresis in the [Li^+]**4** SIC transition was observed causing the [Li^+]**4** to undergo a transition back to its less conductive phase 2 K higher than that at which it was formed. However, hysteresis in the SIC transition temperature of the sodium salt allowed the SIC phase to be stable down to at least 283 K, making it a possible candidate for use in emerging solid-state sodium battery technologies. [Na^+]**4** is still the most conductive SIC material for sodium at room temperature.[176,187]

The collected data were examined to determine trends and design principles in the hope of improving these materials.[171] The improved performance of the *closo*-carboranes **3** and **4**, compared to that of the dianionic borates **1** and **2**, was attributed to (1) the lower cation:anion ratio, (2) the presence of the carbon atom, (3) increased anion reorientations (rotations around their respective C_4 and C_5 axes of symmetry), and (4) weaker Coulombic attractions. A lower cation:anion ratio, in a lattice of approximately the same size, increases the amount of vacancies in that lattice. It is suggested that the increased amount of vacancies lowers the energy of activation for cation diffusion. The presence of the carbon atom on these clusters is expected to lower the phase transition temperatures by increasing the level of intrinsic disorder on the system. Anion reorientations increase from 10^7 to 10^{10} s^{-1} after the SIC transition for the sodium and lithium salts of both **3** and **4**.[172,173] The reorientations are correlated with the phase transition, but it cannot be definitively stated that they aid in the diffusion of cations. Ab initio molecular dynamics calculations show a decrease in conductivity of approximately 3 orders of magnitude, supporting the claim that a more mobile anion leads to increased conductivity.[171] Finally, weaker Coulombic attractions of the carborane anions to their cation counterparts provide a more weakly coordinating environment aiding in the diffusion of cations.

Anion alloying, which is the mixing of different anions with the same cation, is one way to introduce disorder into anion sublattices.[169] This has been shown to lower SIC transition temperatures and to improve conductivity in some cases. Udovic and co-workers investigated anion alloying by mixing **3** and **4** as either their sodium or lithium salts. They reported that an equimolar blend of [Na^+]**3** and [Na^+]**4** lowers the SIC transition temperature, improves conductivity, and inhibits the drastic decline in conductivity below transition temperatures. Similar outcomes were observed for the equimolar mixture of [Li^+]**3** and [Li^+]**4**, except the conductivity of the alloy did not surpass the conductivity of [Li^+]**3** at high temperatures. At 300 K, the lithium carborane mixture had a conductivity that was at least 2 orders of magnitude greater than those of both single salts. However, the conductivity dipped below 10^{-3} S cm^{-1} at approximately 285 K, causing it to no longer be competitive with other Li^+ SIC materials at room temperature.

Carborane anions as solid-state ion-conducting materials are proving to be competitive with other solid-state alternatives; however, this area of research is still in its infancy. There is a lack of research regarding the electrochemistry of complete battery systems. New electrolyte design via cluster functionalization, varying cluster size, and new blends of anions and cations remains unexplored but promising.[188] Additionally, the performance of these anions in polymer matrices and the performance of metal cations other than Na^+ and Li^+ in the solid state have not been investigated.

6. SUMMARY AND OUTLOOK

When Knöth discovered the *closo*-carborane anions **3** and **4**,[21] he likely would not have ever imagined the diverse array of applications these intriguing molecules would find. In the context of nonclassical main group catalysis, it is clear that the future holds more surprises and novel methods enabled by the weakly coordinating and inert properties of these species will continue to emerge. A major challenge for silylium catalysis to become more practical is to devise an approach that would enable greater functional group tolerance. In the realm of transition metal-based catalysis, the unusual ancillary ligands formed by using these clusters themselves or the clusters as ligand substituents create such unique coordination environments that new reactivity patterns will surely be discovered. A future challenge will be to utilize the charge of the carboranes and their weakly coordinating properties to design novel reactions that cannot be attained with traditional transition metal-based catalysts. It also is likely that new radicals that have eluded isolation, such as the triazole radical anion **100**,[149] may be tamed in the future by covalently linking derivatives of **3** and **4**. A future challenge would be to utilize this strategy to produce not only carborane-stabilized radical anions but also radical cations. Given the ever-increasing demand for more sustainable, safer, and more energy dense electrochemical cells, the unmatched electrochemical stability and tunability of **3** and **4** will ensure a bright future for these clusters in energy storage applications. With respect to solid-state ionic conductors, the future challenge will be to design even more ionically conductive materials that display enhanced processability characteristics for device integration.

AUTHOR INFORMATION

Corresponding Authors

*E-mail: masay@chem.ucla.edu.

DOI: 10.1021/acs.chemrev.8b00551
Chem. Rev. XXXX, XXX, XXX−XXX

*E-mail: hosea@chem.ucla.edu.
*E-mail: vincent.lavallo@ucr.edu.

ORCID

J. Guo: 0000-0001-9829-1202
V. Lavallo: 0000-0001-8945-3038

Notes

The authors declare no competing financial interest.

Biographies

Steven Fisher obtained his bachelor's degree in biochemistry from California State University San Marcos in 2013 and is currently working on his PhD at the University of California, Riverside under the supervision of Dr. Vincent Lavallo. His work involves the chemical synthesis of ionic materials featuring boron rich nanoclusters and their use as ligands in organometallic chemistry.

Anton Tomich obtained his B.Sc. in biochemistry from Loyola University Chicago in 2016 and is currently a PhD candidate at University of California, Riverside under the guidance of Dr. Vincent Lavallo. His projects focus on the synthesis of novel electrolyte solutions utilizing carborane anions and their performance in electrochemical devices.

Sergio Lovera graduated from Cal Poly Pomona in 2016 with a Bachelor's of Science in Chemistry. During his time there he worked under Dr. James Rego in developing syntheses of organic molecules as Liquid Crystals. In the summer of 2017 he joined the research group of Dr. Vincent Lavallo at the University of California, Riverside where he is currently working toward his Ph.D. in Chemistry. His project involves the synthesis of carborane anions and their applications as electrolytes.

Jack Kleinsasser was born in Santa Maria, California in 1990. He obtained his bachelors of science in chemistry from Point Loma Nazarene University in San Diego, California in 2013. From there he moved on to work in GE's water and filtration systems division as a production supervisor until beginning to pursue his Ph.D. in Chemistry at the University of California, Riverside under the tutelage of Dr. Vincent Lavallo in 2015. His research interests are in organometallics and catalytic design using carborane appended phosphine ligands.

Juchen Guo earned his Bachelor degree from Zhejiang University in 1999 and his Ph.D. from University of Maryland in 2007, both in Chemical Engineering. From 2007 to 2012, he worked as postdoctoral researcher at University of Maryland (2007 to 2011) and Cornell University (2011 to 2012). He joined the Department of Chemical and Environmental Engineering at University of California, Riverside in summer 2012. His current research interests are interfacial phenomena and material properties in electrochemical energy storage systems including lithium-ion, lithium−sulfur, and multivalent metal ion batteries. He is the recipient of 2014 Hellman Fellowship and 2018 NSF CAREER Award.

Matthew Asay performed his doctoral research at the University of California, Riverside and the University of Paul Sabatier, Toulouse III. Following postdoctoral research stays in Germany as an Alexander von Humboldt fellow and in Japan as a JSPS fellow he performed independent research at the Universidad Nacional Autónoma de México. He is currently researching reactive intermediates at UCLA.

Hosea Nelson was born in San Francisco, California. He first attended City College of San Francisco, before transferring to UC Berkeley, where he earned a Bachelor's degree in chemistry in 2005. He then moved to Caltech where, as both an NSF and a Ford Fellow, he pursued graduate research under the guidance of Prof. Brian Stoltz. During his graduate studies he completed the first total syntheses of trans-taganolides A−D as well as basiliolide B and C. He then moved to UC Berkeley as a UNCF/Merck postdoctoral scholar, where he worked under the tutelage of Prof. F. Dean Toste. There he worked in the area of ion pairing catalysis, developing several methods to forge C−C and C−N bonds with high levels of enantioselectivity. In 2015 he began his independent career at UCLA. There his group uses interdisciplinary strategies to solve problems in several areas including main group catalysis, asymmetric catalysis, biocatalysis, total synthesis and electron microscopy.

Vincent Lavallo was born in Oceanside, California. He first attended Palomar Community College in San Marcos CA, before transferring to UC Riverside, where he earned a Bachelor's degree in Biochemistry in 2005. During his undergraduate years he learned synthetic chemistry in the group of Professor Guy Bertand. Subsequently he stayed at UC Riverside in the Bertrand Group and earned his PhD in chemistry in 2008. During his graduate studies he synthesized the first examples of cyclic alkyl amino carbenes (CAACs), cyclopropenylidenes, and mesoionic carbenes. He then moved to Caltech for a postdoctoral stint in Bob Grubbs's laboratory where he discovered the unprecedented compound $Fe_3(COT)_3$. In 2011 he began his independent career at UC Riverside, focusing on fundamental and applied chemistry of carborane anions, and was promoted to associate professor in 2017.

ACKNOWLEDGMENTS

V.L. and J.G. are grateful to the National Science Foundation for funding this work (Grant DMR-1508537). H.M.N. thanks The David and Lucile Packard Foundation, The Pew Foundation, The Alfred P. Sloan Foundation, and the National Institute of General Medical Sciences (1R35GM128936-01) for generous funding.

REFERENCES

(1) Stock, A. *Hydrides of Boron and Silicon*; Cornell University Press: Ithaca, NY, 1933.
(2) Longuet-Higgins, H. C.; Roberts, M. D. V.; Emeleus, H. J. The Electronic Structure of an Icosahedron of Boron Atoms. *Proc. R. Soc. A* **1955**, *230*, 110−119.
(3) Longuet-Higgins, H. C.; Bell, R. P. The Structure of the Boron Hydrides. *J. Chem. Soc.* **1943**, 250−255.
(4) Lipscomb, W. N. *Boron Hydrides*; Dover Publications: New York, 2013.
(5) Dequasie, A. *The Green Flame: Surviving Government Secrecy*; American Chemical Society: Washington, DC, 1991.
(6) Pitochelli, A. R.; Hawthorne, F. M. The Isolation of The Icosahedral $B_{12}H_{12}^{-2}$ Ion. *J. Am. Chem. Soc.* **1960**, *82*, 3228−3229.
(7) Hawthorne, M. F.; Pitochelli, A. R. The Reaction of Bis-Acetonitrile Decaborane with Amines. *J. Am. Chem. Soc.* **1959**, *81*, 5519−5519.
(8) Spokoyny, A. M. New Ligand Platforms Featuring Boron-rich Clusters as Organomimetic Substituents. *Pure Appl. Chem.* **2013**, *85*, 903−919.
(9) Sivaev, I. V.; Prikaznov, A.; Naoufal, D. Fifty Years of the closo-decaborate Anion Chemistry. *Collect. Czech. Chem. Commun.* **2010**, *75*, 1149−1199.
(10) Sivaev, I.; Bregadze, V.; Sjöberg, S. Chemistry of closo-Dodecaborate Anion $[B_{12}H_{12}]^{2-}$: A Review. *Collect. Czech. Chem. Commun.* **2002**, *67*, 679−727.
(11) Duttwyler, S. Recent Advances in B−H Functionalization of Icosahedral Carboranes and Boranes by Transition Metal Catalysis. *Pure Appl. Chem.* **2018**, *90*, 733.
(12) Eleazer, B. J.; Peryshkov, D. V. Coordination Chemistry of Carborane Clusters: Metal-Boron Bonds in Carborane, Carboranyl, and Carboryne Complexes. *Comments Inorg. Chem.* **2018**, *38*, 79−109.
(13) Grimes, R. N. *Carboranes*; Elsevier: Amsterdam, 2016.

DOI: 10.1021/acs.chemrev.8b00551
Chem. Rev. XXXX, XXX, XXX−XXX

(14) Popescu, A. R.; Teixidor, F.; Viñas, C. Metal Promoted Charge and Hapticities of Phosphines: The Uniqueness of Carboranylphosphines. *Coord. Chem. Rev.* **2014**, *269*, 54−84.
(15) Douvris, C.; Michl, J. Update 1 of: Chemistry of the Carba-*closo*-dodecaborate(−) Anion, $CB_{11}H_{12}^-$. *Chem. Rev.* **2013**, *113*, PR179−PR233.
(16) Olid, D.; Núñez, R.; Viñas, C.; Teixidor, F. Methods to Produce B-C, B-P, B-N and B-S Bonds in Boron Clusters. *Chem. Soc. Rev.* **2013**, *42*, 3318−3336.
(17) Ringstrand, B.; Kaszynski, P. Functionalization of the [*closo*-1-$CB_9H_{10}]^-$ Anion for the Construction of New Classes of Liquid Crystals. *Acc. Chem. Res.* **2013**, *46*, 214−225.
(18) Farras, P.; Juarez-Perez, E. J.; Lepsik, M.; Luque, R.; Núñez, R.; Teixidor, F. Metallacarboranes and their Interactions: Theoretical Insights and their Applicability. *Chem. Soc. Rev.* **2012**, *41*, 3445−3463.
(19) Scholz, M.; Hey-Hawkins, E. Carbaboranes as Pharmacophores: Properties, Synthesis, and Application Strategies. *Chem. Rev.* **2011**, *111*, 7035−7062.
(20) Reed, C. A. $H^+CH_3^+$ and R_3Si^+ Carborane Reagents: When Triflates Fail. *Acc. Chem. Res.* **2010**, *43*, 121−128.
(21) Knoth, W. H. 1-$B_9H_9CH^-$ and $B_{11}H_{11}CH^-$. *J. Am. Chem. Soc.* **1967**, *89*, 1274−1275.
(22) One of the reviewers suggested that the name "caborate" should be used in place of "anionic carborane" or "carborane anion".
(23) Grimes, R. N. Carboranes in the Chemist's Toolbox. *Dalton Trans.* **2015**, *44*, 5939−5956.
(24) Hosmane, N. S.; Eagling, R. *Handbook of Boron Science: With Applications in Organometallics, Catalysis, Materials and Medicine*; World Scientific Publishing Europe Ltd., 2018.
(25) Hosmane, N. S. *Boron Science: New Technologies and Applications*; CRC Press: Boca Raton, FL, 2016.
(26) Knapp, C. In *Weakly Coordinating Anions: Halogenated Borates and Dodecaborates*; Elsevier: Amsterdam, 2013.
(27) Molinos, E.; Brayshaw, S. K.; Kociok-Köhn, G.; Weller, A. S. Sequential Dehydrogenative Borylation/Hydrogenation Route to Polyethyl-Substituted, Weakly Coordinating Carborane Anions. *Organometallics* **2007**, *26*, 2370−2382.
(28) Molinos, E.; Brayshaw, S. K.; Kociok-Kohn, G.; Weller, A. S. Cationic Rhodium mono-Phosphine Fragments Partnered with Carborane Monoanions [*closo*-$CB_{11}H_6X_6]^-$ (X = H, Br). Synthesis, Structures and Reactivity with Alkenes. *Dalton Trans.* **2007**, 4829−4844.
(29) Molinos, E.; Kociok-Köhn, G.; Weller, A. S. Polyethyl Substituted Weakly Coordinating Carborane Anions: a Sequential Dehydrogenative Borylation−hydrogenation Route. *Chem. Commun.* **2005**, 3609−3611.
(30) Rifat, A.; Kociok-Köhn, G.; Steed, J. W.; Weller, A. S. Cationic Iridium Phosphines Partnered with [*closo*-$CB_{11}H_6Br_6]^-$ $(PPh_3)_2Ir(H)_2$(*closo*-$CB_{11}H_6Br_6$) and [$(PPh_3)_2Ir(\eta^2$-$C_2H_4)_3$][*closo*-$CB_{11}H_6Br_6$]. Relevance to Counterion Effects in Olefin Hydrogenation. *Organometallics* **2004**, *23*, 428−432.
(31) Rifat, A.; Patmore, N. J.; Mahon, M. F.; Weller, A. S. Rhodium Phosphines Partnered with the Carborane Monoanions $[CB_{11}H_6Y_6]^-$ (Y = H, Br). Synthesis and Evaluation as Alkene Hydrogenation Catalysts. *Organometallics* **2002**, *21*, 2856−2865.
(32) Weller, A. S.; Mahon, M. F.; Steed, J. W. Rhodium Cyclooctadiene Complexes of the Weakly Coordinating Carborane Anion [*closo*-$CB_{11}H_{12}]^-$Isolation and Crystal Structures of [(COD)-Rh(η^2-$CB_{11}H_{12}$)] and [(COD)Rh$(THF)_2$][$CB_{11}H_{12}$]. *J. Organomet. Chem.* **2000**, *614*−*615*, 113−119.
(33) Mhinzi, G. S.; Litster, S. A.; Redhouse, A. D.; Spencer, J. L. *closo*-Monocarbaboranes as Ligands for Transition Metals: Synthesis and Reactivity of *exo*-diphosphineplatinum-*closo*-monocarbaborane Complexes; Structure of [$Pt\{Bu^{t2}P(CH_2)_2PBu^{t2}\}$(*closo*-$CB_{11}H_{12}$)]-[$CB_{11}H_{12}$]. *J. Chem. Soc., Dalton Trans.* **1991**, 2769−2776.
(34) Omann, L.; Qu, Z.-W.; Irran, E.; Klare, H. F. T.; Grimme, S.; Oestreich, M. Electrophilic Formylation of Arenes by Silylium Ion Mediated Activation of Carbon Monoxide. *Angew. Chem., Int. Ed.* **2018**, *57*, 8301−8305.
(35) Chandra Sheker Reddy, A.; Chen, Z.; Hatanaka, T.; Minami, T.; Hatanaka, Y. Synthesis of Silaoxazolinium Salts Bearing Weakly Coordinating Anions: Structures and Catalytic Activities in the Aldol Reaction. *Organometallics* **2013**, *32*, 3575−3582.
(36) Wehmschulte, R. J.; Saleh, M.; Powell, D. R. CO_2 Activation with Bulky Neutral and Cationic Phenoxyalanes. *Organometallics* **2013**, *32*, 6812−6819.
(37) Schulz, A.; Villinger, A. Tamed" Silylium Ions: Versatile in Catalysis. *Angew. Chem., Int. Ed.* **2012**, *51*, 4526−4528.
(38) Khandelwal, M.; Wehmschulte, R. J. Cationic Organoaluminum Compounds as Intramolecular Hydroamination Catalysts. *J. Organomet. Chem.* **2012**, *696*, 4179−4183.
(39) Ibad, M. F.; Langer, P.; Reiß, F.; Schulz, A.; Villinger, A. Catalytic Trimerization of Bis-silylated Diazomethane. *J. Am. Chem. Soc.* **2012**, *134*, 17757−17768.
(40) Khandelwal, M.; Wehmschulte, R. J. Deoxygenative Reduction of Carbon Dioxide to Methane, Toluene, and Diphenylmethane with $[Et_2Al]^+$ as Catalyst. *Angew. Chem., Int. Ed.* **2012**, *51*, 7323−7326.
(41) Klare, H. F. T.; Oestreich, M. Silylium Ions in Catalysis. *Dalton Trans.* **2010**, *39*, 9176−9184.
(42) Zhang, Y.; Huynh, K.; Manners, I.; Reed, C. A. Ambient Temperature Ring-Opening Polymerisation (ROP) of Cyclic Chlorophosphazene Trimer $[N_3P_3Cl_6]$ Catalyzed by Silylium Ions. *Chem. Commun.* **2008**, 494−496.
(43) Vyakaranam, K.; Barbour, J. B.; Michl, J. Li^+ Catalyzed Radical Polymerization of Simple Terminal Alkenes. *J. Am. Chem. Soc.* **2006**, *128*, 5610−5611.
(44) Kim, K.-C.; Reed, C. A.; Elliott, D. W.; Mueller, L. J.; Tham, F.; Lin, L.; Lambert, J. B. Crystallographic Evidence for a Free Silylium Ion. *Science* **2002**, *297*, 825.
(45) Lambert, J. B.; Zhang, S. Response. *Science* **1994**, *263*, 984−985.
(46) Lambert, J. B.; Olah, G. A.; Rasul, G.; Li, X.-y.; Buchholz, H. A.; Sandford, G.; Prakash, G. K. S. Triethylsilyl Cations. *Science* **1994**, *263*, 983−984.
(47) Lambert, J. B.; Zhang, S.; Stern, C. L.; Huffman, J. C. Crystal Structure of a Silyl Cation with No Coordination to Anion and Distant Coordination to Solvent. *Science* **1993**, *260*, 1917−1918.
(48) Reed, C. A. The Silylium Ion Problem, R_3Si^+Bridging Organic and Inorganic Chemistry. *Acc. Chem. Res.* **1998**, *31*, 325−332.
(49) Lee, V. Y.; Sekiguchi, A. *In Organosilicon Compounds*; Academic Press: New York, 2017.
(50) Reed, C. A. Carboranes: A New Class of Weakly Coordinating Anions for Strong Electrophiles, Oxidants, and Superacids. *Acc. Chem. Res.* **1998**, *31*, 133−139.
(51) Xie, Z.; Manning, J.; Reed, R. W.; Mathur, R.; Boyd, P. D. W.; Benesi, A.; Reed, C. A. Approaching the Silylium (R3Si$^+$) Ion: Trends with Hexahalo (Cl, Br, I) Carboranes as Counterions. *J. Am. Chem. Soc.* **1996**, *118*, 2922−2928.
(52) Klis, T.; Powell, D. R.; Wojtas, L.; Wehmschulte, R. J. Synthesis and Characterization of Bulky Cationic Arylalkylaluminum Compounds. *Organometallics* **2011**, *30*, 2563−2570.
(53) Kim, K.-C.; Reed, C. A.; Long, G. S.; Sen, A. Et2Al+ Alumenium Ion-like Chemistry. Synthesis and Reactivity toward Alkenes and Alkene Oxides. *J. Am. Chem. Soc.* **2002**, *124*, 7662−7663.
(54) Riddlestone, I. M.; Kraft, A.; Schaefer, J.; Krossing, I. Taming the Cationic Beast: Novel Developments in the Synthesis and Application of Weakly Coordinating Anions. *Angew. Chem., Int. Ed.* **2018**, *57*, 13982−14024.
(55) Klare, H. F. T. Catalytic C−H Arylation of Unactivated C−H Bonds by Silylium Ion-Promoted C(sp^2)−F Bond Activation. *ACS Catal.* **2017**, *7*, 6999−7002.
(56) Dagorne, S.; Atwood, D. A. Synthesis, Characterization, and Applications of Group 13 Cationic Compounds. *Chem. Rev.* **2008**, *108*, 4037−4071.
(57) Victor, D. G.; MacDonald, G. J. A Model for Estimating Future Emissions of Sulfur Hexafluoride and Perfluorocarbons. *Clim. Change* **1999**, *42*, 633−662.
(58) Timms, L.; The, P. Chemistry of Volatile Waste from Silicon Wafer Processing. *J. Chem. Soc., Dalton Trans.* **1999**, 815−822.

DOI: 10.1021/acs.chemrev.8b00551
Chem. Rev. XXXX, XXX, XXX−XXX

(59) Lean, J.; Beer, J.; Bradley, R. Reconstruction of Solar Irradiance Since 1610: Implications for Climate Change. *Geophys. Res. Lett.* **1995**, *22*, 3195−3198.
(60) Molina, M. J.; Rowland, F. S. Stratospheric Sink for Chlorofluoromethanes: Chlorine Atom-catalysed Destruction of Ozone. *Nature* **1974**, *249*, 810.
(61) Müller, K.; Faeh, C.; Diederich, F. Fluorine in Pharmaceuticals: Looking Beyond Intuition. *Science* **2007**, *317*, 1881−1886.
(62) Aizenberg, M.; Milstein, D. Homogeneous Rhodium Complex-catalyzed Hydrogenolysis of C-F Bonds. *J. Am. Chem. Soc.* **1995**, *117*, 8674−8675.
(63) Aizenberg, M.; Milstein, D. Catalytic Activation of Carbon-Fluorine Bonds by a Soluble Transition Metal Complex. *Science* **1994**, *265*, 359−361.
(64) Kuehnel, M. F.; Holstein, P.; Kliche, M.; Krüger, J.; Matthies, S.; Nitsch, D.; Schutt, J.; Sparenberg, M.; Lentz, D. Titanium-Catalyzed Vinylic and Allylic CF Bond Activation - Scope, Limitations and Mechanistic Insight. *Chem. - Eur. J.* **2012**, *18*, 10701−10714.
(65) Kuehnel, M. F.; Lentz, D.; Braun, T. Synthesis of Fluorinated Building Blocks by Transition-Metal-Mediated Hydrodefluorination Reactions. *Angew. Chem., Int. Ed.* **2013**, *52*, 3328−3348.
(66) Klahn, M.; Rosenthal, U. An Update on Recent Stoichiometric and Catalytic C−F Bond Cleavage Reactions by Lanthanide and Group 4 Transition-Metal Complexes. *Organometallics* **2012**, *31*, 1235−1244.
(67) Reade, S. P.; Mahon, M. F.; Whittlesey, M. K. Catalytic Hydrodefluorination of Aromatic Fluorocarbons by Ruthenium N-Heterocyclic Carbene Complexes. *J. Am. Chem. Soc.* **2009**, *131*, 1847−1861.
(68) Vela, J.; Smith, J. M.; Yu, Y.; Ketterer, N. A.; Flaschenriem, C. J.; Lachicotte, R. J.; Holland, P. L. Synthesis and Reactivity of Low-Coordinate Iron(II) Fluoride Complexes and Their Use in the Catalytic Hydrodefluorination of Fluorocarbons. *J. Am. Chem. Soc.* **2005**, *127*, 7857−7870.
(69) Young, R. J.; Grushin, V. V. Catalytic C−F Bond Activation of Nonactivated Monofluoroarenes. *Organometallics* **1999**, *18*, 294−296.
(70) Yang, H.; Gao, H.; Angelici, R. J. Hydrodefluorination of Fluorobenzene and 1,2-Difluorobenzene under Mild Conditions over Rhodium Pyridylphosphine and Bipyridyl Complexes Tethered on a Silica-Supported Palladium Catalyst. *Organometallics* **1999**, *18*, 2285−2287.
(71) Gusev, D. G.; Ozerov, O. V. Calculated Hydride and Fluoride Affinities of a Series of Carbenium and Silylium Cations in the Gas Phase and in C_6H_5Cl Solution. *Chem. - Eur. J.* **2011**, *17*, 634−640.
(72) Darwent, B. d. B. *Bond Dissociation Energies In Simple Molecules*; National Bureau of Standards: Washington DC, 1970.
(73) Benson, S. W. III - Bond energies. *J. Chem. Educ.* **1965**, *42*, 502.
(74) Cottrell, T. L. *The Strengths of Chemical Bonds*, 2nd ed.; Butterworths: London, 1958.
(75) Scott, V. J.; Çelenligil-Çetin, R.; Ozerov, O. V. Room-Temperature Catalytic Hydrodefluorination of C(sp^3)−F Bonds. *J. Am. Chem. Soc.* **2005**, *127*, 2852−2853.
(76) Nava, M.; Reed, C. A. Triethylsilyl Perfluoro-Tetraphenylborate, [Et3Si$^+$][F_{20}-BPh4$^-$], a Widely Used Nonexistent Compound. *Organometallics* **2011**, *30*, 4798−4800.
(77) Douvris, C.; Ozerov, O. V. Hydrodefluorination of Perfluoroalkyl Groups Using Silylium-Carborane Catalysts. *Science* **2008**, *321*, 1188−1190.
(78) Douvris, C.; Stoyanov, E. S.; Tham, F. S.; Reed, C. A. Isolating Fluorinated Carbocations. *Chem. Commun.* **2007**, 1145−1147.
(79) Douvris, C.; Nagaraja, C. M.; Chen, C.-H.; Foxman, B. M.; Ozerov, O. V. Hydrodefluorination and Other Hydrodehalogenation of Aliphatic Carbon−Halogen Bonds Using Silylium Catalysis. *J. Am. Chem. Soc.* **2010**, *132*, 4946−4953.
(80) Press, L. P.; McCulloch, B. J.; Gu, W.; Chen, C.-H.; Foxman, B. M.; Ozerov, O. V. Triflyloxy-substituted Carboranes as Useful Weakly Coordinating Anions. *Chem. Commun.* **2015**, *51*, 14034−14037.
(81) Gu, W.; Ozerov, O. V. Exhaustive Chlorination of $[B_{12}H_{12}]^{2-}$ without Chlorine Gas and the Use of $[B_{12}Cl_{12}]_2^-$ as a Supporting Anion in Catalytic Hydrodefluorination of Aliphatic C−F Bonds. *Inorg. Chem.* **2011**, *50*, 2726−2728.
(82) Panisch, R.; Bolte, M.; Müller, T. Hydrogen- and Fluorine-Bridged Disilyl Cations and Their Use in Catalytic C−F Activation. *J. Am. Chem. Soc.* **2006**, *128*, 9676−9682.
(83) Klahn, M.; Fischer, C.; Spannenberg, A.; Rosenthal, U.; Krossing, I. Hydrodefluorination of non-activated C−F Bonds by Diisobutylaluminiumhydride via the Aluminium Cation $[i\text{-}Bu_2Al]^+$. *Tetrahedron Lett.* **2007**, *48*, 8900−8903.
(84) Mallov, I.; Ruddy, A. J.; Zhu, H.; Grimme, S.; Stephan, D. W. Bond Activation by Silylium Cation/Phosphine Frustrated Lewis Pairs: Mono Hydrodefluorination of $PhCF_3PhCF_2H$ and Ph_2CF_2. *Chem. - Eur. J.* **2017**, *23*, 17692−17696.
(85) Chitnis, S. S.; Krischer, F.; Stephan, D. W. Catalytic Hydrodefluorination of C−F Bonds by an Air Stable PIII Lewis Acid. *Chem. - Eur. J.* **2018**, *24*, 6543−6546.
(86) Jones, J. S.; Gabbaï, F. P. Coordination- and Redox-Noninnocent Behavior of Ambiphilic Ligands Containing Antimony. *Acc. Chem. Res.* **2016**, *49*, 857−867.
(87) Bayne, J. M.; Stephan, D. W. Phosphorus Lewis Acids: Emerging Reactivity and Applications in Catalysis. *Chem. Soc. Rev.* **2016**, *45*, 765−774.
(88) Stephan, D. W. Frustrated Lewis Pairs: From Concept to Catalysis. *Acc. Chem. Res.* **2015**, *48*, 306−316.
(89) Price, C. C. *The Alkylation of Aromatic Compounds by the Friedel-Crafts Method*; Wiley & Sons: Hoboken, NJ, 2011.
(90) Friedel, C.; Crafts, J. M. Sur une Nouvelle Méthode Générale de Synthèse d'hydrocarbures, d'acétones, etc. *C. R. Acad. Sci.* **1877**, *84*, 1392.
(91) Duttwyler, S.; Douvris, C.; Fackler, N. L. P.; Tham, F. S.; Reed, C. A.; Baldridge, K. K.; Siegel, J. S. CF Activation of Fluorobenzene by Silylium Carboranes: Evidence for Incipient Phenyl Cation Reactivity. *Angew. Chem., Int. Ed.* **2010**, *49*, 7519−7522.
(92) Allemann, O.; Duttwyler, S.; Romanato, P.; Baldridge, K. K.; Siegel, J. S. Proton-Catalyzed, Silane-Fueled Friedel-Crafts Coupling of Fluoroarenes. *Science* **2011**, *332*, 574−577.
(93) Allemann, O.; Baldridge, K. K.; Siegel, J. S. Intramolecular C-H Insertion vs. Friedel-Crafts Coupling Induced by Silyl Cation-promoted C-F Activation. *Org. Chem. Front.* **2015**, *2*, 1018−1021.
(94) Shao, B.; Bagdasarian, A. L.; Popov, S.; Nelson, H. M. Arylation of Hydrocarbons Enabled by Organosilicon Reagents and Weakly Coordinating Anions. *Science* **2017**, *355*, 1403−1407.
(95) Popov, S.; Shao, B.; Bagdasarian, A. L.; Benton, T. R.; Zou, L.; Yang, Z.; Houk, K. N.; Nelson, H. M. Teaching an Old Carbocation New Tricks: Intermolecular C−H Insertion Reactions of Vinyl Cations. *Science* **2018**, *361*, 381−387.
(96) Gu, W.; Haneline, M. R.; Douvris, C.; Ozerov, O. V. Carbon−Carbon Coupling of C(sp^3)−F Bonds Using Alumenium Catalysis. *J. Am. Chem. Soc.* **2009**, *131*, 11203−11212.
(97) Fein, M. M.; Bobinski, J.; Mayes, N.; Schwartz, N.; Cohen, M. S. Carboranes. I. The Preparation and Chemistry of 1-Isopropenylcarborane and its Derivatives (a New Family of Stable Clovoboranes). *Inorg. Chem.* **1963**, *2*, 1111−1115.
(98) Heying, T. L.; Ager, J. W.; Clark, S. L.; Mangold, D. J.; Goldstein, H. L.; Hillman, M.; Polak, R. J.; Szymanski, J. W. A New Series of Organoboranes. I. Carboranes from the Reaction of Decaborane with Acetylenic Compounds. *Inorg. Chem.* **1963**, *2*, 1089−1092.
(99) Zakharkin, L. I.; Stanko, V. I.; Brattstev, V. A.; Chapovskii, Yu. A.; Struchkov, Tu. T. The Structure of B10C2H12 (Barene) and its Derivatives. *Bull. Acad. Sci. USSR, Div. Chem. Sci.* **1963**, *12*, 1911.
(100) Joost, M.; Zeineddine, A.; Estévez, L.; Mallet-Ladeira, S.; Miqueu, K.; Amgoune, A.; Bourissou, D. Facile Oxidative Addition of Aryl Iodides to Gold(I) by Ligand Design: Bending Turns on Reactivity. *J. Am. Chem. Soc.* **2014**, *136*, 14654−14657.
(101) Joost, M.; Estévez, L.; Mallet-Ladeira, S.; Miqueu, K.; Amgoune, A.; Bourissou, D. Enhanced π-Backdonation from Gold(I): Isolation of Original Carbonyl and Carbene Complexes. *Angew. Chem., Int. Ed.* **2014**, *53*, 14512−14516.

DOI: 10.1021/acs.chemrev.8b00551
Chem. Rev. XXXX, XXX, XXX−XXX

(102) Wang, T.; Duan, Y.; Liu, X.; Xie, Q.; Guo, W.; Yu, X.; Wu, S.; Wang, J.; Liu, G. Retraction of "A 1,2-Dicarbadodecaborane(12)-1,2-Dithiolate Chelating Ruthenium Carbene Catalyst for Highly Z Selective Olefin Metathesis. *Organometallics* **2018**, *37*, 1219−1219.
(103) Ivanov, S. V.; Rockwell, J. J.; Polyakov, O. G.; Gaudinski, C. M.; Anderson, O. P.; Solntsev, K. A.; Strauss, S. H. Highly Fluorinated Weakly Coordinating Monocarborane Anions. 1-H-$CB_{11}F_{11}^-$1-CH_3-$CB_{11}F_{11}^-$ and the Structure of $[N(n\text{-}Bu)_4]_2[CuCl(CB_{11}F_{11})]$. *J. Am. Chem. Soc.* **1998**, *120*, 4224−4225.
(104) Zhang, K.; Shen, Y.; Liu, J.; Spingler, B.; Duttwyler, S. Crystal Structure of a Carborane Endo/Exo-dianion and its use in the Synthesis of Ditopic Ligands for Supramolecular Frameworks. *Chem. Commun.* **2018**, *54*, 1698−1701.
(105) Tsang, C.-W.; Yang, Q.; Mak, T. C. W.; Xie, Z. Synthesis and Crystal Structure of Silver and Argentate Complexes of Mixed Halocarborane Anions, $(C_5H_5N)_2Ag(1\text{-}HCB_{11}Br_5I_6)(C_5H_5N)$ and $[\{(CH_3CN)_4Ag_3\}\{Ag(CB_{11}I_5Br_6)_2\}]$. *Appl. Organomet. Chem.* **2003**, *17*, 449−452.
(106) Hwang, C.-S.; Power, P. P. Synthesis and Characterization of the Lithium Organoargentate Salts $[Li(THF)_4][Ag(Triph)_2]\cdot THF$ and $[Li(THF)_4][Ag(C_6H_3\text{-}2,6\text{-}Mes_2)_2]\cdot 1/8OEt_2$ (Triph = $-C_6H_2$-2,4,6-Ph_3Mes = C_6H_2-2,4,6-Me_3). *J. Organomet. Chem.* **1999**, *589*, 234−238.
(107) Finze, M.; Sprenger, J. A. P. Anionic Gold(I) Complexes—Twelve- and Ten-Vertex Monocarba-*closo*-borate Anions with Carbon−Gold σ Bonds. *Chem. - Eur. J.* **2009**, *15*, 9918−9927.
(108) Wehmschulte, R. J.; Wojtas, L. Cationic Ethylzinc Compound: A Benzene Complex with Catalytic Activity in Hydroamination and Hydrosilylation Reactions. *Inorg. Chem.* **2011**, *50*, 11300−11302.
(109) Walker, D. A.; Woodman, T. J.; Hughes, D. L.; Bochmann, M. Reactions of Zinc Dialkyls with (Perfluorophenyl)boron Compounds: Alkylzinc Cation Formation vs C_6F_5 Transfer. *Organometallics* **2001**, *20*, 3772−3776.
(110) Haufe, M.; Köhn, R. D.; Kociok-Köhn, G.; Filippou, A. C. The Chemistry of 1,3,5-triazacyclohexane Complexes, Synthesis and Structure Determination of Ethyl(−1,3,5-tribenzyl-(−1,3,5-triazacyclohexane)) Zinc(II)-hexafluorophosphate. *Inorg. Chem. Commun.* **1998**, *1*, 263−266.
(111) Himmelspach, A.; Sprenger, J. A. P.; Warneke, J.; Zähres, M.; Finze, M. Mercury(II) Complexes of the Carba-*closo*-dodecaboranyl Ligands $[closo\text{-}1\text{-}CB_{11}X_{11}]^{2-}$ (X = H, F, Cl, Br, I). *Organometallics* **2012**, *31*, 1566−1577.
(112) Himmelspach, A.; Zähres, M.; Finze, M. Salts of the Lewis-Acidic Dianion $[Hg(closo\text{-}1\text{-}CB_{11}F_{11})_2]^{2-}$Coordination of Acetonitrile and Water. *Inorg. Chem.* **2011**, *50*, 3186−3188.
(113) Himmelspach, A.; Warneke, J.; Schäfer, M.; Hailmann, M.; Finze, M. Salts of the Dianions $[Hg(12\text{-}X\text{-}closo\text{-}1\text{-}CB_{11}H_{10})_2]^{2-}$ (X = I, C≡CH, C≡CFc, C≡CSiiPr$_3$): Synthesis and Spectroscopic and Structural Characterization. *Organometallics* **2015**, *34*, 462−469.
(114) Himmelspach, A.; Finze, M.; Raub, S. Tetrahedral Gold(I) Clusters with Carba-*closo*-dodecaboranylethynido Ligands: $[\{12\text{-}(R_3PAu)_2C{\square}C\text{-}closo\text{-}1\text{-}CB_{11}H_{11}\}_2]$. *Angew. Chem., Int. Ed.* **2011**, *50*, 2628−2631.
(115) Schäfer, M.; Krummenacher, I.; Braunschweig, H.; Finze, M. Boron Clusters with a Ferrocenylalkynyl Group Bonded to Boron: Synthesis, Characterization, and Electrochemical Trends. *Z. Anorg. Allg. Chem.* **2015**, *641*, 660−668.
(116) Himmelspach, A.; Finze, M. Ethynylmonocarba-*closo*-dodecaborates: $M[12\text{-}HCC\text{-}closo\text{-}1\text{-}CB_{11}H_{11}]$ and $M[7,12\text{-}(HCC)_2\text{-}closo\text{-}1\text{-}CB_{11}H_{10}]$ (M = $Cs^+[Et_4N]^+$). *J. Organomet. Chem.* **2010**, *695*, 1337−1345.
(117) Finze, M. Carba-*closo*-dodecaborates with One or Two Alkynyl Substituents Bonded to Boron. *Inorg. Chem.* **2008**, *47*, 11857−11867.
(118) Hailmann, M.; Wolf, N.; Renner, R.; Hupp, B.; Steffen, A.; Finze, M. Silver(I) Clusters with Carba-*closo*-dodecaboranylethynyl Ligands: Synthesis, Structure, and Phosphorescence. *Chem. - Eur. J.* **2017**, *23*, 11684−11693.
(119) Hailmann, M.; Wolf, N.; Renner, R.; Schäfer, T. C.; Hupp, B.; Steffen, A.; Finze, M. Unprecedented Efficient Structure Controlled Phosphorescence of Silver(I) Clusters Stabilized by Carba-*closo*-dodecaboranylethynyl Ligands. *Angew. Chem., Int. Ed.* **2016**, *55*, 10507−10511.
(120) Wolf, N.; Hailmann, M.; Finze, M. Silver(I) Complexes of 12-Phenylalkynyl- and 12-Triisopropylalkynylcarba-*closo*-dodecaborate Anions. *Eur. J. Inorg. Chem.* **2017**, *2017*, 4459−4466.
(121) Shen, Y.; Liu, J.; Sattasatchuchana, T.; Baldridge, K. K.; Duttwyler, S. Transition Metal Complexes of a Monocarba-*closo*-dodecaborate Ligand via B−H Activation. *Eur. J. Inorg. Chem.* **2017**, *2017*, 4420−4424.
(122) Shen, Y.; Pan, Y.; Liu, J.; Sattasathuchana, T.; Baldridge, K. K.; Duttwyler, S. Synthesis and Full Characterization of an Iridium B−H Activation Intermediate of the Monocarba-*closo*-dodecaborate Anion. *Chem. Commun.* **2017**, *53*, 176−179.
(123) Jelinek, T.; Baldwin, P.; Scheidt, W. R.; Reed, C. A. New Weakly Coordinating Anions. 2. Derivatization of the Carborane Anion $CB_{11}H_{12}$. *Inorg. Chem.* **1993**, *32*, 1982−1990.
(124) Nava, M. J.; Reed, C. A. High Yield C-Derivatization of Weakly Coordinating Carborane Anions. *Inorg. Chem.* **2010**, *49*, 4726−4728.
(125) Drisch, M.; Sprenger, J. A. P.; Finze, M. Carba-closo-dodecaborate Anions with Cluster Carbon−Phosphorous Bonds. *Z. Anorg. Allg. Chem.* **2013**, *639*, 1134−1139.
(126) Röhrscheid, F.; Holm, R. H. Zero-valent Nickel Complexes of Bis(phosphino)-*o*-carboranes. *J. Organomet. Chem.* **1965**, *4*, 335−338.
(127) Zakharkin, L. I.; Kalinin, V. N.; Snyakin, A. P.; Kvasov, B. A. Effect of Solvents on the Electronic Properties of 1-*o*-, 3-*o*- and 1-*m*-carboranyl groups. *J. Organomet. Chem.* **1969**, *18*, 19−26.
(128) Spokoyny, A. M.; Lewis, C. D.; Teverovskiy, G.; Buchwald, S. L. Extremely Electron-Rich, Boron-Functionalized, Icosahedral Carborane-Based Phosphinoboranes. *Organometallics* **2012**, *31*, 8478−8481.
(129) Spokoyny, A. M.; Machan, C. W.; Clingerman, D. J.; Rosen, M. S.; Wiester, M. J.; Kennedy, R. D.; Stern, C. L.; Sarjeant, A. A.; Mirkin, C. A. A Coordination Chemistry Dichotomy for Icosahedral Carborane-based Ligands. *Nat. Chem.* **2011**, *3*, 590−596.
(130) Estrada, J.; Lugo, C. A.; McArthur, S. G.; Lavallo, V. Inductive Effects of 10 and 12-Vertex *closo*-Carborane Anions: Cluster Size and Charge Make a Difference. *Chem. Commun.* **2016**, *52*, 1824−1826.
(131) El-Hellani, A.; Kefalidis, C. E.; Tham, F. S.; Maron, L.; Lavallo, V. Structure and Bonding of a Zwitterionic Iridium Complex Supported by a Phosphine with the Parent Carba-*closo*-dodecaborate $CB_{11}H_{11}^-$ Ligand Substituent. *Organometallics* **2013**, *32*, 6887−6890.
(132) Estrada, J.; Lee, S. E.; McArthur, S. G.; El-Hellani, A.; Tham, F. S.; Lavallo, V. Resisting B−H Oxidative Addition: The Divergent Reactivity of the *o*-carborane and Carba-*closo*-dodecaborate Ligand Substituents. *J. Organomet. Chem.* **2015**, *798*, 214−217.
(133) Arthur, T. S.; Glans, P.-A.; Singh, N.; Tutusaus, O.; Nie, K.; Liu, Y.-S.; Mizuno, F.; Guo, J.; Alsem, D. H.; Salmon, N. J.; Mohtadi, R. Interfacial Insight from Operando XAS/TEM for Magnesium Metal Deposition with Borohydride Electrolytes. *Chem. Mater.* **2017**, *29*, 7183−7188.
(134) Lavallo, V.; Wright, J. H.; Tham, F. S.; Quinlivan, S. Perhalogenated Carba-*closo*-dodecaborate Anions as Ligand Substituents: Applications in Gold Catalysis. *Angew. Chem., Int. Ed.* **2013**, *52*, 3172−3176.
(135) Estrada, J.; Woen, D. H.; Tham, F. S.; Miyake, G. M.; Lavallo, V. Synthesis and Reactivity of a Zwitterionic Palladium Allyl Complex Supported by a Perchlorinated Carboranyl Phosphine. *Inorg. Chem.* **2015**, *54*, 5142−5144.
(136) Nakamura, A.; Anselment, T. M. J.; Claverie, J.; Goodall, B.; Jordan, R. F.; Mecking, S.; Rieger, B.; Sen, A.; van Leeuwen, P. W. N. M.; Nozaki, K. *Ortho*-Phosphinobenzenesulfonate: A Superb Ligand for Palladium-Catalyzed Coordination−Insertion Copolymerization of Polar Vinyl Monomers. *Acc. Chem. Res.* **2013**, *46*, 1438−1449.
(137) Chan, A. L.; Estrada, J.; Kefalidis, C. E.; Lavallo, V. Changing the Charge: Electrostatic Effects in Pd-Catalyzed Cross-Coupling. *Organometallics* **2016**, *35*, 3257−3260.
(138) Biscoe, M. R.; Fors, B. P.; Buchwald, S. L. A New Class of Easily Activated Palladium Precatalysts for Facile C−N Cross-Coupling Reactions and the Low Temperature Oxidative Addition of Aryl Chlorides. *J. Am. Chem. Soc.* **2008**, *130*, 6686−6687.

DOI: 10.1021/acs.chemrev.8b00551
Chem. Rev. XXXX, XXX, XXX−XXX

(139) Barder, T. E.; Biscoe, M. R.; Buchwald, S. L. Structural Insights into Active Catalyst Structures and Oxidative Addition to (Biaryl)-phosphine−Palladium Complexes via Density Functional Theory and Experimental Studies. *Organometallics* **2007**, *26*, 2183−2192.
(140) Estrada, J.; Lavallo, V. Fusing Dicarbollide Ions with N Heterocyclic Carbenes. *Angew. Chem., Int. Ed.* **2017**, *56*, 9906−9909.
(141) Asay, M. J.; Fisher, S. P.; Lee, S. E.; Tham, F. S.; Borchardt, D.; Lavallo, V. Synthesis of Unsymmetrical N-carboranyl NHCs: Directing Effect of the Carborane Anion. *Chem. Commun.* **2015**, *51*, 5359−5362.
(142) El-Hellani, A.; Lavallo, V. Fusing N-Heterocyclic Carbenes with Carborane Anions. *Angew. Chem., Int. Ed.* **2014**, *53*, 4489−4493.
(143) Jelínek, T.; Plešek, J.; Heřmánek, S.; Štíbr, B. Chemistry of Compounds with the 1-Carba-*closo*-dodecaborane(12) Framework. *Collect. Czech. Chem. Commun.* **1986**, *51*, 819−929.
(144) Aldeco-Perez, E.; Rosenthal, A. J.; Donnadieu, B.; Parameswaran, P.; Frenking, G.; Bertrand, G. Isolation of a C5-Deprotonated Imidazolium, a Crystalline "Abnormal" N-Heterocyclic Carbene. *Science* **2009**, *326*, 556−559.
(145) Wang, Y.; Xie, Y.; Abraham, M. Y.; Wei, P.; Schaefer, H. F.; Schleyer, P. v. R.; Robinson, G. H. A Viable Anionic N-Heterocyclic Dicarbene. *J. Am. Chem. Soc.* **2010**, *132*, 14370−14372.
(146) Hawthorne, M. F.; Young, D. C.; Wegner, P. A. Carbametallic Boron Hydride Derivatives. I. Apparent Analogs of Ferrocene and Ferricinium Ion. *J. Am. Chem. Soc.* **1965**, *87*, 1818−1819.
(147) Fisher, S. P.; El-Hellani, A.; Tham, F. S.; Lavallo, V. Anionic and Zwitterionic Carboranyl N-heterocyclic Carbene Au(I) Complexes. *Dalton Trans.* **2016**, *45*, 9762−9765.
(148) Clavier, H.; Nolan, S. P. Percent Buried Volume for Phosphine and N-heterocyclic Carbene Ligands: Steric Properties in Organometallic Chemistry. *Chem. Commun.* **2010**, *46*, 841−861.
(149) Asay, M.; Kefalidis, C. E.; Estrada, J.; Weinberger, D. S.; Wright, J.; Moore, C. E.; Rheingold, A. L.; Maron, L.; Lavallo, V. Isolation of a Carborane-Fused Triazole Radical Anion. *Angew. Chem., Int. Ed.* **2013**, *52*, 11560−11563.
(150) Wright, J. H.; Kefalidis, C. E.; Tham, F. S.; Maron, L.; Lavallo, V. Click-Like Reactions with the Inert $HCB_{11}Cl_{11}^-$ Anion Lead to Carborane-Fused Heterocycles with Unusual Aromatic Character. *Inorg. Chem.* **2013**, *52*, 6223−6229.
(151) Chan, A. L.; Fajardo, J.; Wright, J. H.; Asay, M.; Lavallo, V. Observation of Room Temperature B−Cl Activation of the $HCB_{11}Cl_{11}^-$ Anion and Isolation of a Stable Anionic Carboranyl Phosphazide. *Inorg. Chem.* **2013**, *52*, 12308−12310.
(152) Boeré, R. T.; Bolli, C.; Finze, M.; Himmelspach, A.; Knapp, C.; Roemmele, T. L. Quantum-Chemical and Electrochemical Investigation of the Electrochemical Windows of Halogenated Carborate Anions. *Chem. - Eur. J.* **2013**, *19*, 1784−1795.
(153) Jow, R. T.; Xu, K.; Borodin, O.; Makoto, U. *Electrolytes for Lithium and Lithium-ion Batteries*; Springer: New York, 2016.
(154) Tutusaus, O.; Mohtadi, R.; Arthur, T. S.; Mizuno, F.; Nelson, E. G.; Sevryugina, Y. V. An Efficient Halogen-Free Electrolyte for Use in Rechargeable Magnesium Batteries. *Angew. Chem., Int. Ed.* **2015**, *54*, 7900−7904.
(155) Tang, W. S.; Unemoto, A.; Zhou, W.; Stavila, V.; Matsuo, M.; Wu, H.; Orimo, S.-i.; Udovic, T. J. Unparalleled Lithium and Sodium Superionic Conduction in Solid Electrolytes with Large Monovalent Cage-like Anions. *Energy Environ. Sci.* **2015**, *8*, 3637−3645.
(156) Tutusaus, O.; Mohtadi, R.; Singh, N.; Arthur, T. S.; Mizuno, F. Study of Electrochemical Phenomena Observed at the Mg Metal/Electrolyte Interface. *ACS Energy Lett.* **2017**, *2*, 224−229.
(157) McArthur, S. G.; Jay, R.; Geng, L.; Guo, J.; Lavallo, V. Below the 12-vertex: 10-vertex Carborane Anions as non-Corrosive, Halide Free, Electrolytes for Rechargeable Mg Batteries. *Chem. Commun.* **2017**, *53*, 4453−4456.
(158) McArthur, S. G.; Geng, L.; Guo, J.; Lavallo, V. Cation Reduction and Comproportionation as Novel Strategies to Produce High Voltage, Halide Free, Carborane Based Electrolytes for Rechargeable Mg Batteries. *Inorg. Chem. Front.* **2015**, *2*, 1101−1104.
(159) Hahn, N. T.; Seguin, T. J.; Lau, K.-C.; Liao, C.; Ingram, B. J.; Persson, K. A.; Zavadil, K. R. Enhanced Stability of the Carba-*closo*-dodecaborate Anion for High-Voltage Battery Electrolytes through Rational Design. *J. Am. Chem. Soc.* **2018**, *140*, 11076−11084.
(160) Rajput, N. N.; Seguin, T. J.; Wood, B. M.; Qu, X.; Persson, K. A. Elucidating Solvation Structures for Rational Design of Multivalent Electrolytes—A Review. *Top. Curr. Chem.* **2018**, *376*, 19.
(161) Aurbach, D.; Lu, Z.; Schechter, A.; Gofer, Y.; Gizbar, H.; Turgeman, R.; Cohen, Y.; Moshkovich, M.; Levi, E. Prototype Systems for Rechargeable Magnesium Batteries. *Nature* **2000**, *407*, 724−727.
(162) Choi, J. W.; Aurbach, D. Promise and Reality of Post-lithium-ion Batteries with High Energy Densities. *Nat. Rev. Mater.* **2016**, *1*, 16013.
(163) Bucur, C. B.; Gregory, T.; Oliver, A. G.; Muldoon, J. Confession of a Magnesium Battery. *J. Phys. Chem. Lett.* **2015**, *6*, 3578−3591.
(164) Mohtadi, R.; Mizuno, F. Magnesium Batteries: Current State of the Art, Issues and Future Perspectives. *Beilstein J. Nanotechnol.* **2014**, *5*, 1291−1311.
(165) Muldoon, J.; Bucur, C. B.; Gregory, T. Quest for Nonaqueous Multivalent Secondary Batteries: Magnesium and Beyond. *Chem. Rev.* **2014**, *114*, 11683−11720.
(166) Yoo, H. D.; Shterenberg, I.; Gofer, Y.; Gershinsky, G.; Pour, N.; Aurbach, D. Mg Rechargeable Batteries: an On-going Challenge. *Energy Environ. Sci.* **2013**, *6*, 2265−2279.
(167) Muldoon, J.; Bucur, C. B.; Oliver, A. G.; Sugimoto, T.; Matsui, M.; Kim, H. S.; Allred, G. D.; Zajicek, J.; Kotani, Y. Electrolyte Roadblocks to a Magnesium Rechargeable Battery. *Energy Environ. Sci.* **2012**, *5*, 5941−5950.
(168) Kim, H. S.; Arthur, T. S.; Allred, G. D.; Zajicek, J.; Newman, J. G.; Rodnyansky, A. E.; Oliver, A. G.; Boggess, W. C.; Muldoon, J. Structure and Compatibility of a Magnesium Electrolyte with a Sulphur Cathode. *Nat. Commun.* **2011**, *2*, 427.
(169) Tang, W. S.; Yoshida, K.; Soloninin, A. V.; Skoryunov, R. V.; Babanova, O. A.; Skripov, A. V.; Dimitrievska, M.; Stavila, V.; Orimo, S.-i.; Udovic, T. J. Stabilizing Superionic-Conducting Structures via Mixed-Anion Solid Solutions of Monocarba-*closo*-borate Salts. *ACS Energy Lett.* **2016**, *1*, 659−664.
(170) Tang, W. S.; Matsuo, M.; Wu, H.; Stavila, V.; Zhou, W.; Talin, A. A.; Soloninin, A. V.; Skoryunov, R. V.; Babanova, O. A.; Skripov, A. V.; Unemoto, A.; Orimo, S.-I.; Udovic, T. J. Liquid-Like Ionic Conduction in Solid Lithium and Sodium Monocarba-*closo*-Decaborates Near or at Room Temperature. *Adv. Energy Mater.* **2016**, *6*, 1502237.
(171) Varley, J. B.; Kweon, K.; Mehta, P.; Shea, P.; Heo, T. W.; Udovic, T. J.; Stavila, V.; Wood, B. C. Understanding Ionic Conductivity Trends in Polyborane Solid Electrolytes from Ab Initio Molecular Dynamics. *ACS Energy Lett.* **2017**, *2*, 250−255.
(172) Soloninin, A. V.; Dimitrievska, M.; Skoryunov, R. V.; Babanova, O. A.; Skripov, A. V.; Tang, W. S.; Stavila, V.; Orimo, S.-i.; Udovic, T. J. Comparison of Anion Reorientational Dynamics in MCB_9H_{10} and $M_2B_{10}H_{10}$ (M = Li, Na) via Nuclear Magnetic Resonance and Quasielastic Neutron Scattering Studies. *J. Phys. Chem. C* **2017**, *121*, 1000−1012.
(173) Skripov, A. V.; Skoryunov, R. V.; Soloninin, A. V.; Babanova, O. A.; Tang, W. S.; Stavila, V.; Udovic, T. J. Anion Reorientations and Cation Diffusion in $LiCB_{11}H_{12}$ and $NaCB_{11}H_{12}$ ^{1}H, ^{7}Li, and ^{23}Na NMR Studies. *J. Phys. Chem. C* **2015**, *119*, 26912−26918.
(174) Zheng, F.; Kotobuki, M.; Song, S.; Lai, M. O.; Lu, L. Review on Solid Electrolytes for All-Solid-State Lithium-Ion Batteries. *J. Power Sources* **2018**, *389*, 198−213.
(175) Gao, Z.; Sun, H.; Fu, L.; Ye, F.; Zhang, Y.; Luo, W.; Huang, Y. Promises, Challenges, and Recent Progress of Inorganic Solid-State Electrolytes for All-Solid-State Lithium Batteries. *Adv. Mater.* **2018**, *30*, 1705702.
(176) Zhao, C.; Liu, L.; Qi, X.; Lu, Y.; Wu, F.; Zhao, J.; Yu, Y.; Hu, Y.-S.; Chen, L. Solid-State Sodium Batteries. *Adv. Energy Mater.* **2018**, *8*, 1703012.
(177) Wang, Y.; Richards, W. D.; Ong, S. P.; Miara, L. J.; Kim, J. C.; Mo, Y.; Ceder, G. Design Principles for Solid-State Lithium Superionic Conductors. *Nat. Mater.* **2015**, *14*, 1026.

DOI: 10.1021/acs.chemrev.8b00551
Chem. Rev. XXXX, XXX, XXX−XXX

(178) Zhang, H.; Li, C.; Piszcz, M.; Coya, E.; Rojo, T.; Rodriguez-Martinez, L. M.; Armand, M.; Zhou, Z. Single Lithium-Ion Conducting solid Polymer Electrolytes: Advances and Perspectives. *Chem. Soc. Rev.* **2017**, *46*, 797−815.
(179) Wiersema, R. J.; Hawthorne, M. F. Electrochemistry and Boron-11 Nuclear Magnetic Resonance Spectra of Monocarbon Carboranes. *Inorg. Chem.* **1973**, *12*, 785−788.
(180) He, X.; Zhu, Y.; Mo, Y. Origin of Fast Ion Diffusion in Superionic Conductors. *Nat. Commun.* **2017**, *8*, 15893.
(181) Kweon, K. E.; Varley, J. B.; Shea, P.; Adelstein, N.; Mehta, P.; Heo, T. W.; Udovic, T. J.; Stavila, V.; Wood, B. C. Structural, Chemical, and Dynamical Frustration: Origins of Superionic Conductivity in *closo*-Borate Solid Electrolytes. *Chem. Mater.* **2017**, *29*, 9142−9153.
(182) Unemoto, A.; Ikeshoji, T.; Yasaku, S.; Matsuo, M.; Stavila, V.; Udovic, T. J.; Orimo, S.-i. Stable Interface Formation between TiS_2 and $LiBH_4$ in Bulk-Type All-Solid-State Lithium Batteries. *Chem. Mater.* **2015**, *27*, 5407−5416.
(183) Udovic, T. J.; Matsuo, M.; Unemoto, A.; Verdal, N.; Stavila, V.; Skripov, A. V.; Rush, J. J.; Takamura, H.; Orimo, S.-i. Sodium Superionic Conduction in $Na_2B_{12}H_{12}$. *Chem. Commun.* **2014**, *50*, 3750−3752.
(184) Udovic, T. J.; Matsuo, M.; Tang, W. S.; Wu, H.; Stavila, V.; Soloninin, A. V.; Skoryunov, R. V.; Babanova, O. A.; Skripov, A. V.; Rush, J. J.; Unemoto, A.; Takamura, H.; Orimo, S.-i. Exceptional Superionic Conductivity in Disordered Sodium Decahydro-*closo*-decaborate. *Adv. Mater.* **2014**, *26*, 7622−7626.
(185) Núñez, R.; Tarrés, M.; Ferrer-Ugalde, A.; de Biani, F. F.; Teixidor, F. Electrochemistry and Photoluminescence of Icosahedral Carboranes, Boranes, Metallacarboranes, and Their Derivatives. *Chem. Rev.* **2016**, *116*, 14307−14378.
(186) Arntson, K. S.; Langley, M. B. A Phenomenological Theory for Hysteresis in the Ionic Conductivity of Solid Electrolytes. *Phys. Status Solidi A* **1982**, *69*, 185−192.
(187) Song, S.; Duong, H. M.; Korsunsky, A. M.; Hu, N.; Lu, L. A Na^+ Superionic Conductor for Room-Temperature Sodium Batteries. *Sci. Rep.* **2016**, *6*, 32330.
(188) Zhong, M.; Zhou, J.; Fang, H.; Jena, P. Role of Ligands in the Stability of B_nX_n and $CB_n{-}1X_n$ (n = 5−10; X = H, F, CN) and their Potential as Building Blocks of Electrolytes in Lithium Ion Batteries. *Phys. Chem. Chem. Phys.* **2017**, *19*, 17937−17943.

DOI: 10.1021/acs.chemrev.8b00551
Chem. Rev. XXXX, XXX, XXX−XXX